

ELUCIDATION OF BINDING SITES OF DUAL ANTAGONISTS IN THE HUMAN CHEMOKINE RECEPTORS CCR2 AND CCR5.

Spencer E. Hall¹, Allen Mao¹, Vicky Nicolaidou, Mattea Finelli, Emma L. Wise, Belinda Nedjai, Julie Kanjanapangka, Paymann Harirchian, Deborah Chen, Victor Selchau, Sofia Ribeiro, Sabine Schyler, James E. Pease, Richard Horuk and Nagarajan Vaidehi*
Department of Immunology Beckman Research Institute of the City of Hope (S.E.H., A.M., J.K., N.V)

Leukocyte Biology Section, National Heart and Lung Institute, Imperial College London, London SW7 2AZ, United Kingdom (V.N., M.F., E.L.W., B.N., J.E.P.)
Berlex Biosciences, Richmond, (P.H., D.C., V.S., S.R., S.S., R.H.)

A. Running Title: Antagonist binding sites in CCR2 and CCR5

B. Address correspondence to: Nagarajan Vaidehi, Beckman Research Institute of the City of Hope, 1500 E. Duarte Road, Duarte, CA-91010. Telephone: (626)-301-8408; Fax: (626)-301-8186; E-mail: NVaidehi@coh.org

C. Number of pages of text excluding abstract = 23 pages

Number of tables = 4

Number of Figures = 6

Number of References = 40

Number of words in the abstract = 221

Number of words in the Introduction = 689 (including references)

Number of words in the Discussion = 1713

D. Abbreviations used

GPCR – G-Protein Coupled Receptor;

TM - transmembrane

Abstract

Design of dual antagonists for the chemokine receptors CCR2 and CCR5 will be greatly facilitated by knowledge of the structural differences of their binding sites. Thus, we computationally predicted the binding site of the dual CCR2/CCR5 antagonist TAK-779, with the chemical name N,N-Dimethyl-N-[4-[[[2-(4-methylphenyl)-6,7-dihydro-5H-benzohepten-8-yl] carbonyl]amino]benzyl]tetrahydro-2H-pyran-4-aminium, and a CCR2 specific antagonist Teijin compound 1 (with the chemical name N-(carbamoylmethyl)- 3-trifluoromethyl benzamido- parachlorobenzyl 3-aminopyrrolidine) in an ensemble of predicted structures of human CCR2 and CCR5. Based on our predictions of the protein-ligand interactions, we examined the activity of the antagonists for cells expressing thirteen mutants of CCR2 and five mutants of CCR5. The results show that residues W98^{2.60} and T292^{7.40} contribute significantly to the efficacy of both TAK-779 and Teijin compound 1, while by contrast H121^{3.33} and I263^{6.55} contribute significantly only to the antagonistic effect of Teijin compound 1 at CCR2. Mutation of residues W86^{2.60} and Y108^{3.32} adversely affected the efficacy of TAK-779 in antagonizing CCR5-mediated chemotaxis. Y49A^{1.39} and E291A^{7.39} mutants of CCR2 showed a complete loss of CCL2 binding and chemotaxis, despite robust cell surface expression, suggesting that these residues are critical in maintaining the correct receptor architecture. Modeling studies support the hypothesis that the residues Y49^{1.39}, W98^{2.60}, Y120^{3.32}, and E291^{7.39} of CCR2 form a tight network of aromatic cluster and polar contacts between transmembrane helices 1, 2, 3 and 7.

Introduction

The chemokine receptors CCR2 and CCR5 are G protein-coupled receptors (GPCRs) and share around 73% sequence identity mainly in their transmembrane (TM) helices (Charo et al 1994, Samson et al 1996). CCR2 is mainly expressed in monocytes, immature dendritic cells, activated T-lymphocytes and basophils, and binds several chemokines, CCL2, CCL7, CCL8 and CCL13 (Murphy 1994). CCR5 is expressed by both CD4+ and CD8+ activated T-lymphocytes and monocytes and has three high affinity ligands, CCL3, CCL4 and CCL5 (Doms and Peiper 1997). Both CCR2 and CCR5 and their ligands have been implicated in the pathophysiology of a number of diseases, including rheumatoid arthritis, and multiple sclerosis (Szekanecz et al 2006, Charo and Ransohoff 2006).

Based on their roles in disease, chemokine receptors have been attractive targets for the pharmaceutical industry. Unfortunately despite a massive effort and numerous clinical trials so far only one registered drug, the CCR5 antagonist Mariviroc/Selzentry, has resulted from this approach (Lieberman-Blum et al 2008). The lack of success of chemokine receptor antagonists in the clinic may be due in part to receptor redundancy and this could explain why these small molecule antagonists, specific for a single receptor, did not provide a therapeutic effect (Ribeiro and Horuk 2005). It has been suggested that promiscuous compounds that target more than one receptor might be therapeutically more effective for treating these complex multi-factorial diseases (Morphy and Rankovic, 2005, Frantz 2005).

Knowledge of the structural basis of chemokine receptor subtype selectivity, and the receptor conformations stabilized by dual antagonists could help facilitate the design of novel chemokine receptor antagonists. For this reason we have modeled an ensemble of low energy three-dimensional receptor conformations of human CCR2 and CCR5 receptors using the MembStruk4.0 computational method (Hall 2005, Heo et al 2007) and predicted the binding sites

of a CCR2/CCR5 dual antagonist, N,N-Dimethyl-N-[4-[[[2-(4-methylphenyl)-6,7-dihydro-5H-benzohepten-8-yl] carbonyl]amino]benzyl]tetrahydro-2H-pyran-4-aminium also known as TAK-779 (Baba et al 1999), and a CCR2 specific compound N-(carbamoylmethyl)- 3-trifluoromethyl benzamido- parachlorobenzyl 3-aminopyrrolidine from Teijin, (described as Teijin compound 1) (Moree et al 2008). The residues in the predicted antagonist binding sites of each receptor were subsequently validated using site-directed mutagenesis, and following transient expression, chemotaxis measurements, and radio-labeled chemokine competitive binding experiments were carried out.

Using the class A GPCR numbering system proposed by Ballesteros and Weinstein (Ballesteros and Weinstein 1995) we find that the conserved residue W98^{2.60} (W86^{2.60} in CCR5) contributes significantly to the antagonistic efficacy of TAK-779 in both CCR2 and CCR5, while the effect of H121^{3.33} on TAK-779 in CCR2 is replaced by Y108^{3.32} in CCR5. The rotational orientation of TM3 is different in CCR2 and CCR5 models, thus positioning these important conserved aromatic residues differently. Comparing the binding sites of TAK-779 and Teijin compound 1 in CCR2, we find that the residues I263^{6.55} and T292^{7.40} in CCR2 contribute significantly to binding of Teijin compound 1 in CCR2 but not to TAK-779. Residue E291^{7.39} in TM7, a highly conserved residue in many CC chemokine receptors, contributes substantially to binding of the protonated Teijin compound 1, and CCL2 but not to the quaternary amine antagonist TAK-779. H121^{3.33} on TM3 and Ile263^{6.55} on TM6 also strongly interact with Teijin compound 1, but only weakly with TAK-779. These differences in the binding of a quaternary and tertiary amine antagonist were predicted by our structural models of CCR2 and subsequently verified by point mutation studies.

MOL# 53470

We conclude from this study that E291^{7.39} can position TM7 in different orientations thereby generating different receptor conformations. Based on the data from these studies we postulate that the inter-helical contacts E291^{7.39}, Y49^{1.39}, W98^{2.60} and Y120^{3.32} in CCR2 form a receptor activation network. This interaction network between TMs 1, 2, 3 and 7 is formed when E291^{7.39} faces TM1 and TM2. We observe that this network is present in our models of the CCR5, CCR3 and CCR1 receptors as well. We hypothesize that this network is required for activation by the chemokine. From our studies, we conclude that an alternative conformation (in which E291^{7.39} is facing TM3 and TM6) is stabilized by antagonist binding. Thus the variation in the position of E^{7.39} leads to the multiple receptor conformations observed in both CCR2 and CCR5.

Materials and Methods

Materials: Recombinant human CCL2 and CCL3 were from Peprotech EC (London, UK). ¹²⁵I-Labeled CCL2 and CCL3 were obtained from PerkinElmer Life Sciences (Waltham, MA). The monoclonal anti-HA antibody was purchased from Cambridge Bioscience (Cambridge, UK). Fluorescein isothiocyanate-conjugated goat anti-mouse antibody was purchased from DakoCytomation (Ely, UK). All other reagents were purchased from Sigma-Aldrich (Poole, UK) and Invitrogen (Paisley, UK), unless stated otherwise. The CCR2 specific antagonist (Teijin compound 1) shown in Fig. 1, was synthesized as described previously (Moree et al 2008). TAK-779 [Repository number ARP968] was obtained from the Programme EVA Centre for AIDS Reagents, NIBSC, UK, supported by the EC FP6/7 Europrise Network of Excellence, AVIP and NGIN consortia and the Bill and Melinda Gates GHRC-CAVD Project and was donated by NIAID, distributed with the permission of Takeda Chemical Industries, Ltd.

Molecular modeling using the MembStruk4.0 - The MembStruk4.0 procedure used in this work has been published in detail previously (Hall 2005, Heo et al 2008). Here we describe briefly the methods as applied to CCR2 and CCR5.

The seven TM regions and the hydrophobic maxima for each helix in human CCR2 and CCR5 were predicted using the TM2ndS method (Trabanino et al 2004). The TM2ndS uses a multiple sequence alignment that includes all human, rat and mouse chemokine receptor CCR and some of the CXCR sequences, and predicts the TM region based on the seven maxima in hydrophobicity over the entire sequence alignment. The predicted seven TM regions for both CCR2 and CCR5 are shown in Scheme 1 in the supplementary material.

The next step was to optimize the rotation, translation and the helical kinks starting from an assembled bundle of the canonical helices built from the TM predictions. Canonical right-

handed α -helices were built for each helix and their helical axes were oriented in space according to the 7.5 Å low resolution electron density map of frog rhodopsin (Schertler, 1998). This 7.5 Å electron density map gives the positions and the rough relative orientations of the helical axes that serves as the starting point for optimization of the helical bundle. It should be emphasized here that no information was used from any of the crystal structures of GPCRs. The relative translational orientation of the seven helices was optimized by aligning the hydrophobic maximum determined for each helix, to a plane. The rotational orientation was optimized using a combination of hydrophobic moments and molecular dynamics techniques. More details of the procedure are given in the supplementary material. Thus using the MembStruk4.0 procedure we derived an ensemble of low energy TM barrel conformations for both CCR2 and CCR5. The receptor conformations were chosen by maximum number of interhelical hydrogen bonds, and the best total energy of the protein conformation in explicit lipid bilayer. The two low energy conformations chosen for CCR2 differ in the rotational orientations of TM7 that leads to different orientations of the conserved residues E291^{7.39} and T292^{7.40}. In CCR5, two energetically favorable rotational orientations were found for TM6 and TM7, giving rise to four possible receptor conformations. We selected the receptor conformation with the best score with respect to the number of inter-helical hydrogen bonds and the total potential energy of the receptor in explicit lipid bilayer. Extra- and intracellular loops were added using *Whatif* (Vriend 1990) and the second extra-cellular loop (ECL) was added using the ECL2 loop of bovine rhodopsin (pdb code: 1hzx).

Prediction of the binding site for the antagonists TAK-779 and Teijin compound 1: The antagonists modeled in this study are shown in Fig. 1. We built the ligands using the “*LigPrep*”

module in the Glide suite from Schrodinger Inc. Multiple ligand conformations were generated for each of the two ligands using the Monte Carlo method embedded in *MacroModel* (Schrodinger Inc.). The ligand conformations were clustered using a 1.0 Å RMSD cutoff in coordinates, and the lowest energy conformation from each cluster was selected for docking. Each conformation of the ligands was docked using *Glide SP* (Schrodinger Inc); the top scoring 10 docked conformations were saved and filtered using a cutoff of 80% in ligand buried surface area. The conformations were further refined using *MacroModel's Redundant Conformer Elimination*, varying the RMSD between conformations to reduce the number of clusters of conformations. Next, we performed a complete conjugate gradient minimization of the protein and ligand to 0.1 kcal/mol/Å RMS in force/atom. We then selected all residues within 5.0Å of the ligand and optimized them using the side chain optimizer in *Prime* (Schrodinger Inc). The conformations were scored by the binding energies calculated as

$$BE = PE (\text{ligand in fixed protein}) - PE (\text{ligand in solvation}),$$

where BE is the binding energy, PE (ligand in fixed protein) is the potential energy of the ligand calculated with the protein atoms fixed, and PE (ligand in solvation) is the potential energy of the ligand calculated with the Surface Generalized Born continuum solvation method (Ghosh et al 1998). The best scoring docked conformation(s) were then visually inspected. Lastly, we calculated the contribution of each residue within 5.0 Å of the ligand to the interaction energy of ligand with the receptor.

Generation of receptor mutants and their transient expression in L1.2 cells - pcDNA3.1 plasmids containing human CCR2 and human CCR5 with a 6xHAepitope tag at the N-terminus were purchased from the Missouri S&T cDNA Resource Center (www.cdna.org). These were

subsequently used as a template for the generation of point mutants by polymerase chain reaction (PCR) using the QuikChange II site-directed mutagenesis kit (Stratagene, Amsterdam, Netherlands) and appropriate oligonucleotide primers. All mutants were verified by DNA sequencing (MWG Biotech, Ebersberg, Germany) prior to use. The murine pre-B lymphoid cell line L1.2 cells was maintained as described previously (Vaidehi et al 2006, de Mendonca et al 2005) in suspension at 37 °C with 5% CO₂ at a density of no more than 1 x 10⁶ cells/ml. Plasmids were introduced into L1.2 cells by electroporation as previously described (Vaidehi et al 2006) which allows for transient, high-level expression of chemokine receptors in a relevant leukocyte background following overnight incubation with 10 mM sodium butyrate.

Flow cytometry - Transient transfectants were assessed for cell surface expression by flow cytometry following staining with an anti-HA antibody and FITC-conjugated secondary antibody as previously described (Vaidehi et al 2006).

Chemotaxis assay - ChemoTx™ plates (Neuroprobe, Gaithersburg, MD) were used as described previously (Vaidehi et al 2006) with chemokine placed into the bottom wells in a final volume of 31 µl of chemotaxis media (HEPES-modified RPMI 1640 media containing 0.1% bovine serum albumin). A 5 µm pore filter was placed on top of the wells, and 2 x 10⁵ cells in a volume of 20 µl of chemotaxis media were loaded onto the filter. Following incubation for 5 h in a humidified chamber at 37 °C with 5% CO₂, cells were scraped from the upper surface of the filter, the filter removed and the migrating cells spun into a white opaque plate using a 96-well funnel plate (Neuroprobe). Cells were counted as previously described (Stroke et al 2006) by the addition of 30µl of CellTiter Glo dye (Promega, Southampton, UK) and luminescence measured using a

Topcount scintillation counter (Perkin Elmer Life Sciences). In some assays a fixed concentration of chemokine was employed in the lower well in the presence or absence of different concentrations of the small molecule antagonists TAK-779 and Teijin compound 1. Migration was reported as the chemotactic index, defined as the ratio of chemokine-driven cell migration to migration to buffer alone. In every experiment, cells transiently expressing WT constructs were employed as a positive control.

Radiolabeled chemokine binding studies: Whole cell binding assays on transiently transfected L1.2 cells were performed as described previously (Vaidehi et al 2006, de Mendonca et al 2005) using 0.1 nM of radiolabeled ligand and increasing concentrations of unlabeled homologous chemokine or antagonist. The parameters we used for the binding assays fit the conditions recommended by Daugherty et al 2000. Briefly, all dilutions were carried out in binding buffer (0.1 % BSA and 0.05 % NaN₃ in RPMI). Previously transfected L1.2 cells were resuspended at 0.5×10^6 cells/25 μ L in binding buffer and 25 μ L of cells were incubated with 5 μ L of 1 nM ¹²⁵I-CCL2 (CCR2 transfectants) or 5 μ L of 1 nM ¹²⁵I-CCL3 (CCR5 transfectants) together with 20 μ L of varying concentrations of unlabelled competing chemokine or antagonist. Binding was allowed to proceed at room temperature for 60 minutes after which 50 μ L of salt wash (0.4 g NaCl in 10 mL of binding buffer) was added to each well. The samples were then mixed and layered onto 100 μ L of Nyosil oil in a spate tube and cells were pelleted through the oil by centrifugation at 8500 rpm, for 3 minutes. Cell associated radioactivity was counted in a Canberra Packard Cobra 5010 γ counter (Canberra Packard, Pangebourne, UK). Curve fitting and subsequent data analysis was carried out using the program PRISM and IC₅₀ values were obtained by nonlinear regression analysis (GraphPad Software, Inc., San Diego, CA). In all

MOL# 53470

experiments, each data point was assayed in duplicate. Data are presented as the percentage of counts obtained in the absence of cold competing ligand.

Results

Comparison of the Inter-helical Contacts of the Predicted Structures of CCR2 and CCR5: Fig. 2A shows that in the apo-protein structural model of CCR2 there is a hydrogen bond between D88^{2.50} and N60^{1.50}, and a long (possibly water mediated) hydrogen bond (8.0 Å) with N301^{7.49}. This network of hydrogen bonds is highly conserved across class A GPCRs, and has been observed in both, the rhodopsin and the β 2 adrenergic receptor crystal structures (Palczewski et al 2000, Cherezov et al 2007). The CCR5 apo-protein structural model also forms a hydrogen bond between N48^{1.50} and D76^{2.50} and between D76^{2.50} and N293^{7.49}, albeit with increased heavy atom distances between H-bond partners compared to those in CCR2 (Fig. 2B). Additionally, we observe a rhodopsin-like inter-helical hydrogen bond between W165^{4.50} (W153^{4.50} in CCR5) and N83^{2.45} (N71^{2.45} in CCR5), as shown in Figs. 2A and 2B.

Our predicted structural models for CCR2 and CCR5 reveal that the TXP motif on TM2, that is conserved in many chemokine receptors including CCR2 and CCR5 (Govaerts et al 2003), results in a proline kink that points towards TM3 (shown in Fig. S2 of the Supplementary material). This kink angle is modulated over a range of 15° to 47° in CCR2 and 17° to 40° in CCR5, as seen from the molecular dynamics simulation of these helices. In contrast, in the rhodopsin sequence the TXP motif is replaced by a GGF motif that places TM2 toward TM7 (Palczewski et al 2000), similar to the β 2 adrenergic receptor (Cherezov et al 2007).

W256^{6.48} (W248^{6.48} in CCR5), a highly conserved residue in class A GPCRs, forms an intra-helical hydrogen bond with N260^{6.52} (N252^{6.52} in CCR5) on TM6. Y120^{3.32} (Y108^{3.32} in CCR5) and Y124^{3.36} (F112^{3.36} in CCR5) on TM3 aid in stabilizing the receptors through aromatic ring stacking. There is also an inter-helical aromatic ring stacking between W256^{6.48} (W248^{6.48} in CCR5) and Y120^{3.32} (Y108^{3.32} in CCR5). We find that the aromatic rings of W98^{2.60} and

Y49^{1.39} do not stack in CCR2 while they do in the CCR5 structural model. The position of E291^{7.39} is variable in the ensemble of structures. There are two positions for E291^{7.39} in CCR2, one where E291^{7.39} is directed towards TM1 and TM2, while in the other conformation E291^{7.39} is facing TM3. Depending on which of these conformations is preferred for E291^{7.39}, the position of N301^{7.49} on TM7 makes or breaks an inter-helical hydrogen bond with TM2. Similarly, there are two possible orientations of TM7 in CCR5. In the first orientation, E283^{7.39} forms inter-helical hydrogen bonds with Y37^{1.39} and Y108^{3.32}. In this orientation of TM7, N293^{7.49} faces TM6 and forms possibly a water-mediated inter-helical hydrogen bond with D76^{2.50} on TM2, as described above. The second orientation of TM7 in CCR5 places E283^{7.39} towards TM3, retaining the inter-helical hydrogen bond with Y108^{3.32} and breaking the hydrogen bond with Y37^{1.39}. Y37^{1.39} and W86^{2.60} stabilize inter-helical interactions with a tight inter-helical aromatic stacking interaction.

Predicted binding site of Teijin compound 1 and TAK 779 in CCR2: The predicted binding site of Teijin compound 1 and TAK-779 in CCR2 are shown in Fig. 3A and 3B. The binding site of the CCR2-specific Teijin compound 1 is located between TM1, TM2, TM3, TM6 and TM7. Fig. 3C shows the residues within 5 Å of Teijin compound 1 in CCR2. The strongest protein-ligand interaction according to our energy calculations, stems from the electrostatic interaction between E291^{7.39} and the pyrrolidine nitrogen (distance 2.8 Å). The calculated pKa for this group (*Jaguar*, Schrodinger Inc) is 7.8 at pH 7.0. T292^{7.40} makes a hydrogen bond with the backbone carbonyl group next to the trifluoro phenyl ring. Residues Y49^{1.39}, W98^{2.60}, Y120^{3.32}, H121^{3.33}, W256^{6.48}, N260^{6.52}, I263^{6.55}, contribute about 1 to 5 kcal/mol of favorable non-bonded

interaction energy and the dominant contributions among these interactions are van der Waals interaction between the antagonist and W98^{2.60}, Y120^{3.32} and H121^{3.33}.

Predicted binding site of TAK-779 antagonist in CCR2: The binding site of TAK-779 in both CCR2 and CCR5 is located between TM1, TM2, TM3, TM6, and TM7, as shown for CCR2 in Figs. 3A and B. The residues that interact strongly with TAK-779 in CCR2 are shown in Fig. 3D. The strength of the electrostatic interaction of the quaternary amine group of TAK-779 with E291^{7.39} is significantly weaker than the interaction with the tertiary amine of Teijin compound 1. The interaction energy of TAK-779 with T292^{7.40}, W98^{2.60}, Y120^{3.32} and H121^{3.33} are similar to that of Teijin compound 1. Additionally, I263^{6.55} interacts favorably only with Teijin compound 1 and not with TAK-779. Although the overall interaction energy of Teijin compound 1 with the CCR2 receptor is more favorable, its desolvation penalty lowers its overall predicted binding affinity compared to TAK-779. We predict that the aromatic cluster of Y49^{1.39}, W98^{2.60}, Y120^{3.32}, H121^{3.33}, Y124^{3.36}, and W256^{6.48} is a major contributor to the interaction between CCR2 and TAK779.

Experimental validation of predicted binding sites of Teijin compound 1 and TAK-779 in CCR2

Surface expression of mutant CCR2: To verify the predicted binding sites for TAK-779 and Teijin compound 1, we constructed a series of mutants based on our predictions. These mutants include key residues predicted to be in the binding pocket, such as: Y49A^{1.39}, W98A^{2.60}, F116A^{3.28}, Y120A^{3.32}, H121A^{3.33}, Y124A^{3.36}, F125A^{3.37}, W256A^{6.48}, I263A^{6.55}, E291A^{7.39}, E291Q^{7.39}, and T292V^{7.40}. Cells transfected with the WT receptor or with mutants such as I208A^{5.44}, which is not in the predicted binding site for either compound, served as controls. The

point mutants, with the exception of F116A^{3.28}, Y124A^{3.36} and W256A^{6.48} were all transiently expressed at high levels on the surface of L1.2 cells as detected by flow cytometry after incubation with an antibody to an epitope tag at the receptor amino-terminus (Fig. 4A). In the CCR2 model the residues Y124^{3.36} and W256^{6.48} form inter-helical aromatic interactions that confer stability to the receptor conformation. Mutation of one of these residues has the potential to break this inter-helical contact and render the protein misfolded. F116^{3.28} pi-stacks with W98^{2.60} in TM2 in CCR2, and hence its mutation to alanine may destabilize the receptor, resulting in a lack of expression. Previous CCR2 structure-function studies did not include mutations of F116^{3.28}, Y124^{3.36} or W256^{6.48} (Berkhout et al 2003, Mirzadegan et al 2000).

Chemotaxis experiments of functional point mutants of CCR2: The same transfectants were subsequently used in chemotaxis assays to assess the effects of mutation on CCR2 function (Fig. 4B). The majority of transfectants behaved similarly to those expressing WT CCR2, exhibiting the bell-shaped concentration response curve typical of these assays, with a maximum response to 1 nM CCL2. The Y120A^{3.32} construct mediated detectable responses at 10 nM and 100 nM CCL2, whilst Y49A^{1.39} was unresponsive across the entire CCL2 concentration range tested. The point-mutant E291A^{7.39} was unresponsive in chemotaxis, despite being expressed at levels significantly greater than those of WT CCR2. The E291Q^{7.39} mutation restored some of the chemotactic response, suggesting that both the charge and size of this amino acid are critical for receptor activation by the ligand. Cells expressing the F116A^{3.28}, Y124A^{3.36} and W256A^{6.48} mutants were unresponsive to all concentrations of CCL2 tested, most likely as a consequence of little or no cell surface expression (data not shown). We observe that the mutants I208A^{5.44}, I263A^{6.55} and T292V^{7.40} have comparable surface expression levels to WT CCR2, but show

greater efficacy in chemotaxis assays. This may be a consequence of GPCR activation being catalytic in nature, and therefore small but detectable decreases in cell surface expression levels will have little effect on downstream signaling as manifested in a chemotaxis assay.

Measurements of Chemotaxis dependence on the antagonist concentration in functional mutants of CCR2: The ability of TAK-779 and Teijin compound 1 to inhibit CCL2-mediated chemotaxis in functional mutants of CCR2 was tested. As predicted by molecular modeling, Teijin compound 1 had a reduced ability to inhibit CCL2-mediated chemotaxis of transfectants expressing the H121A^{3.33}, I263A^{6.55} and T292V^{7.40} point mutants of CCR2, resulting in significantly reduced IC₅₀ values (Fig. 4C and Table 1). Teijin compound 1 had a reduced ability to inhibit CCL2-mediated chemotaxis of transfectants expressing mutants W98A^{2.60}, and E291Q^{7.39} (Fig. 4E) at higher concentrations of CCL2 (10 nM to 100 nM). In contrast, for TAK-779 only cells expressing the T292V^{7.40} and W98A^{2.60} constructs showed a significantly reduced inhibitory response, with IC₅₀ values of 415 nM and 142 nM respectively, compared to an IC₅₀ value of 6 nM for WT CCR2 transfectants (Figs. 4D and 4F and Table 1).

Displacement of radiolabeled CCL2 measurements for TAK-779 and Teijin compound 1: To consolidate the data, the ability of each mutant to bind radiolabeled CCL2 was also examined. The resulting IC₅₀ values from these measurements are shown in Table 2. The ability of the Teijin compound 1 to displace ¹²⁵I-CCL2 from transfectants expressing the H121A^{3.33}, I263A^{6.55} and T292V^{7.40} mutants was significantly reduced, in accordance with the chemotaxis data for these mutants. Likewise, the ability of TAK-779 to displace ¹²⁵I-CCL2 from cells expressing the T292V^{7.40} mutant was significantly diminished (IC₅₀ of 664 nM compared to 49 nM for WT

CCR2), in agreement with the chemotaxis data. No specific binding of the ^{125}I -CCL2 to cells expressing the Y49A^{1.39}, W98A^{2.60}, Y120A^{3.32} and E291Q^{7.39} mutants was observed, suggesting that mutation lowered the affinity of CCL2 for the receptor beyond the limits of detection in this assay.

In the predicted structure, residues H121^{3.33} and I263^{6.55} show favorable van der Waals interactions with the 2,4-dimethylphenyl moiety (see Fig. 3C) of Teijin compound 1. T292^{7.40} forms a hydrogen bond with the carbonyl attached to the trifluorotoluidyl ring. This is in agreement with the significant change in the IC_{50} values obtained with Teijin compound 1 and transfectants expressing H121A^{3.33}, I263A^{6.55} and T292V^{7.40} mutants. . The CCR2 residue E291^{7.39} shows strong electrostatic interactions with the pyrrolidine nitrogen (calculated pKa using Jaguar from Schrodinger Inc is 7.8 at 7.0 pH) and this is in agreement with the observed two orders of magnitude reduction in the antagonistic effect of Teijin compound 1 in chemotaxis assays using 10 nM of CCL2 to drive chemotaxis of cells expressing the E291Q^{7.39} mutant. Although specific binding of ^{125}I -CCL2 to cells expressing the CCR2 mutant W98A^{2.60} was undetectable (Table 2) the same transfectants showed reduced sensitivity to Teijin compound 1 in chemotaxis assays employing an increased concentration of CCL2 (10nM). In contrast the transfectants expressing the F125A^{3.37} and I208A^{5.44} mutants did not show any significant change in the IC_{50} values, as we predicted. Similarly, mutation of I208A^{5.44} had little effect on sensitivity to either antagonist, in agreement with our predictions that it lay outside the antagonist binding site.

Iterative process between predictions and experiments: The predicted structure of TAK-779 in CCR2 shows favorable hydrogen bond interactions of T292^{7.40} with the oxygen on the

tetrahydropyran ring (see Fig. 3D). The predicted binding site is in agreement with experiments with respect to the location of the quaternary amine, tetrahydropyran and the central phenyl ring. However, contrary to the predictions, H121A^{3.33}, F125A^{3.37} and I263A^{6.55} did not show significant changes in the IC₅₀ of TAK-779. These data led to the conclusion that we had predicted the binding interactions for the quaternary amine group of TAK-779, the associated tetrahydropyran and the central phenyl ring correctly, but not for the benzocycloheptenyl and the terminal tolyl moieties. Subsequently, we clustered the docked ligand conformations according to their diversity in conformation of the benzocycloheptenyl and tolyl moieties and chose the docked conformation with the best binding energy. In this docking pose, the terminal tolyl ring points away from H121^{3.33}, F125^{3.37} and Y120^{3.32}, as indicated by the mutation studies.

Predicted Binding site of the TAK-779 antagonist in CCR5: The predicted binding site of TAK-779 in CCR5 is shown in Figs. 5A and 5B, and the residues that interact strongly with TAK-779 are shown in Fig. 5C. TAK-779 interacts with TM1, TM2, TM3, TM6 and TM7. E283^{7.39} has favorable long range Coulombic interactions with the ligand, in analogy with E291^{7.39} in CCR2. It should be noted that this long range Coulombic interaction is not as favorable as the interaction of E291^{7.39} with the Teijin compound 1 in CCR2. Residues W86^{2.60}, Y108^{3.32}, and T284^{7.40} contribute between 2 to 5 kcal/mol to the binding energy. In addition, L104^{3.28} and T105^{3.29} also show favorable but weaker van der Waals interactions. The distance between F109^{3.33} and F112^{3.36} and the terminal tolyl ring of TAK-779 is around 4.5 Å. Residue Y37^{1.39} pi-stacks with W86^{2.60}, which in turn interacts with the quaternary amine group of TAK-779. We find that the contribution of T284^{7.40} to the interaction with the TAK-779 is significantly less in CCR5 than in

CCR2 (T292^{7.40}). We picked the top 5 mutations sorted by their interaction energies with TAK-779, which is in the order E283^{7.39} > Y108^{3.32} > F109^{3.33} > Y37^{1.39} > W86^{2.60}.

Experimental validation of the predicted binding site for TAK-779 in CCR5

Surface Expression and Chemotaxis measurements of point mutants of CCR5 to CCL3: A panel of CCR5 point mutants were expressed transiently in L1.2 cells. Fig. 6A shows the cell surface expression of the constructs relative to that of WT CCR5 as deduced by flow cytometry. Unlike CCR2, CCR5 was more tolerant to point mutations; with only the W86A^{2.60} and Y108A^{3.32} mutations resulting in modest reductions in cell surface expression. The same transfectants were subsequently used in chemotaxis assays to assess the effects of mutation on receptor function (Fig. 6B). The majority of transfectants behaved as those expressing WT CCR5, exhibiting bell-shaped dose response curves with a maximum response to 30 nM CCL3. Notably, the cells expressing the Y37A^{1.39} mutant of CCR5 were completely unresponsive to CCL3 across the concentration range of CCL3 examined.

Modeling suggests that Y37^{1.39} in TM1 pi-stacks with W86^{2.60} on TM2, and therefore the Y37A^{1.39} mutation may lead to a receptor conformation which prevents CCL3 binding and activation. The importance of the aromatic residues in CCR5 was also highlighted by a previous study (Govaerts et al 2003), which suggested that several aromatic residues within TM 2, 3 and 6 formed important intra- and inter-helical contacts, responsible for maintaining an active receptor conformation. In contrast, cells expressing the F109A^{3.33} construct were responsive to CCL3 and exhibited a left-shifted dose-response curve compared to cells expressing WT CCR5, suggesting the mutant receptor had higher affinity for CCL3 than the WT receptor (see Table 3). This was

confirmed by homologous competition binding assays in which ^{125}I -CCL3 was displaced by unlabelled CCL3 from cells expressing either WT or mutant CCR5 (Table 4).

Measurements on concentration dependence of antagonism in functional mutants of CCR5:

Functional mutants were then assessed for their ability to be antagonized by TAK-779 in chemotaxis assays using a fixed concentration of 30 nM CCL3 (Fig. 6C). As predicted by modeling, cells expressing the W86A^{2.60} and Y108A^{3.32} mutants showed a large rightward shift in the concentration-response curve, indicative of a significantly reduced sensitivity to antagonism by TAK-779. In contrast, the F109A^{3.33} and E283Q^{7.39} mutations, had little effect on the potency of TAK-779 compared to WT CCR5, with a modest increase in IC₅₀ values (Table 4). Notable were the findings that the W86A^{2.60} and Y108A^{3.32} constructs exhibited a loss in TAK-779 activity of greater than two orders of magnitude. The ability of TAK-779 to displace ^{125}I -CCL3 from each mutant was also examined. Supportive of the chemotaxis data, in ^{125}I -CCL3 binding studies cells expressing the W86A^{2.60}, Y108A^{3.32}, F109A^{3.33} and E283Q^{7.39} constructs exhibited reduced sensitivity to TAK-779 compared to WT CCR5, with W86A^{2.60} and Y108A^{3.32} transfectants showing the greatest loss of sensitivity to the antagonist (Table 4).

In contrast to Teijin compound 1, we predicted that E291^{7.39} would have little effect on the IC₅₀ of TAK-779 in both CCR2 and CCR5. This is because the quaternary amines of the compound can interact favorably with aromatic residues through cation- π interactions (Gallivan and Dougherty 1999) rather than forming a salt bridge. This is in complete agreement with our data where the E283Q^{7.39} mutant (which retains the polar nature of the glutamate residue) does not significantly affect TAK-779 antagonist activity. In the predicted binding model of TAK-779 in CCR5 (Fig. 5C), W86^{2.60} has favorable cation- π interactions with the quaternary amine

MOL# 53470

group on TAK-779, and indeed mutation of W86^{2,60} resulted in the largest change in IC₅₀. Residue Y108^{3,32} shows favorable van der Waals interactions with both the central phenyl and cycloheptenyl ring of TAK-779, and mutation of this residue significantly lowers its IC₅₀ value 70-fold.

Discussion

Lack of Chemotaxis by some CCR2 and CCR5 mutants: Cells expressing the CCR2 point mutants Y49A^{1.39}, and E291A^{7.39} showed no detectable CCL2 binding and no chemotactic responses to CCL2, while the mutants W98A^{2.60}, Y120A^{3.32}, E291Q^{7.39} showed chemotactic responses only at relatively high concentrations of CCL2 (10nM to 100nM) and no specific binding of 0.1nM ¹²⁵I-CCL2 (Tables 1 and 2). In contrast, the corresponding mutants in CCR5, with the exception of Y37A^{1.39}, showed binding and chemotactic response to CCL3. Interestingly, the Y37A^{1.39} mutant of CCR5 does show activity in HIV viral entry studies (Seibert et al 2006, Dragic et al 2000). How can we account for the lack of response of these CCR2 mutants, given their expression at comparable levels to the wild type receptors? Studies have shown that residues in the amino terminus of several chemokines are required for inducing signaling through their respective receptors (Allen et al 2007). For example, truncation of the amino-terminus of CCL2 converts it into a high affinity antagonist for CCR2 (Gong and Clark-Lewis 1995, Zhang and Rollins 1995, Jarnagin et al 1999). Thus, we hypothesize that the first few residues in the amino terminus of CCL2 interact with residues Y49^{1.39}, W98^{2.60}, Y120^{3.32} and E291^{7.39} in CCR2 in the active receptor state. Residues Y49^{1.39} (Y37^{1.39} in CCR5), W98^{2.60} (W86^{2.60} in CCR5), Y120^{3.32} (Y108^{3.32} in CCR5), and E291^{7.39} (E283^{7.39} in CCR5) form a tight inter-helical network as observed in the models of both CCR2 and CCR5 (Fig. S1 A and B of the supplementary material). The amino-terminus of CCL2 activates CCR2 by strengthening this inter-helical network since the second residue in CCL2 which is a Lys could form a strong salt bridge with E291^{7.39} in CCR2, and trigger receptor activation. This residue is a Gln in CCL3 and therefore the receptor mutation E283Q^{7.39} in CCR5 does not affect the activation of CCR5 by CCL3. Thus based on our experimental and modeling data we postulate that the inter-helical

contacts observed in the region between E291^{7.39}, Y49^{1.39}, W98^{2.60} and Y120^{3.32} form an essential network stabilizing the receptor in the active state while the antagonists like Teijin and TAK-779 bind to disrupt this network and lock it in an inactive conformation.

Binding Site of TAK-779 in CCR2 and CCR5: Table 5 shows the list of residues we have found to be important in binding of the two antagonists in both CCR2 and CCR5. Comparisons of the effect of mutation upon the binding site of TAK-779 in both CCR2 and CCR5 show that the residues W98^{2.60} of CCR2 and W86^{2.60} in CCR5 are both utilized by TAK-779. In contrast, TAK-779 contacts Y108^{3.32} of CCR5 but not Y120^{3.32} of CCR2. Residues H121^{3.33} (F109^{3.33} in CCR5), and E291^{7.39} (E283^{7.39} in CCR5) are not utilized by TAK-779 to antagonize either CCR2 or CCR5, but are used by Teijin compound 1 to antagonize CCR2.

TAK-779 is a dual antagonist with 1 nM binding affinity for CCR5 and 27 nM for CCR2 (Baba et al 1999). Examination of the functional groups of TAK-779 that interact with particular residues, shows that the charge of the quaternary amine in TAK-779 is delocalized on the alkyl substituents, leading to predicted preferred interactions with the aromatic residues Y49^{1.39}, W98^{2.60}, Y120^{3.32} in CCR2 and Y37^{1.39}, W86^{2.60} and Y108^{3.32} in CCR5, rather than forming a salt bridge with E291^{7.39} (E283^{7.39} in CCR5). The benzocycloheptenyl moiety of TAK-779 is buried in the TM regions of CCR2, while in CCR5 it points toward ECL2 (Fig. S3). The terminal tolyl moiety of TAK-779 has a similar location in both CCR2 and CCR5. Thus, although the overall binding site for TAK-779 is similar in CCR2 and CCR5, the contributions of individual amino acids to antagonist binding vary.

Binding Site of Teijin compound 1 and TAK-779 in CCR2: The binding site of both TAK-779 and Teijin compound 1 in CCR2 is located between TM1, TM2, TM3, TM6 and TM7. Although the antagonists share a binding region, the energy contribution of certain residues to ligand binding is different. This difference in contribution could be due to side chain orientation or difference in ligand orientation. Residues W98^{2.60} and T292^{7.40} contribute differentially to binding of TAK-779 and Teijin compound 1, whereas residues H121^{3.33}, E291^{7.39}, and I263^{6.55} contribute only to Teijin compound 1 and have very negligible contributions to TAK-779 as shown in Table 5. In CCR2, E291^{7.39} contributes less to TAK-779 than to Teijin compound 1 binding (Berkhout et al 2003). Also the orientation of E291^{7.39} differs in the TAK-779 and the Teijin compound 1 bound CCR2 structures. We believe that subtype selectivity of Teijin compound 1 for CCR2 could arise from the differential contributions from residues H121^{3.33}, I263^{6.55}, and E291^{7.39}. One pitfall that we have observed in the CCR2 model is that Y120^{3.32} was predicted to have significant interaction with both Teijin compound 1 and TAK-779 in CCR2. Mutation suggested that this is not the case. We believe that Y120^{3.32} may still have an effect on the binding of other antagonists and the effect of the ligand-induced conformational changes in the receptor upon binding could allow Y120^{3.32} to move out of the binding pocket for TAK-779 and Teijin compound 1. Work to study these conformational changes using the computational methods described in Bhattacharya et al (Bhattacharya et al 2008) is underway.

Comparison of the antagonist binding site in CCR2 and CCR5 to other CCR chemokine receptors and other class A GPCRs: Although the residues shown to be important for antagonist activity in CCR2 and CCR5 may not be strictly extrapolated to other chemokine receptors and class A GPCRs, we have attempted to put these results in perspective for sake of comparison.

Table 6 shows a comparison of relative importance of various residues in the binding pocket of antagonists studied for the four chemokine receptors, CCR1, CCR2, CCR3 and CCR5. Y1.39, Y3.32 and W2.60 are conserved across CCR1 to CCR9 chemokine receptors. Y1.39 and Y3.32 have significant effect on either agonist or antagonist binding in all the four CCR1 (de Mendonca et al 2005), CCR2 (Berkhout et al 2003), CCR3 (Wise et al 2007) and CCR5 (Dragic et al 2000, Maeda et al 2006, Seibert et al 2006) chemokine receptors, and W2.60 has significant effect on antagonist inhibition only in CCR2 and CCR5. Based on our models of these four receptors we observed that W2.60 is positioned more in the inter-helical region between TM2 and TM3 in CCR1 and CCR3 and inside the binding pocket in CCR5. In the CCR2 model W2.60 is well positioned towards the ligand for Teijin compound 1 binding and not for TAK-779. H3.33 is not strictly conserved in all the four chemokine receptors, but have significant effect on antagonist inhibition in CCR1 and CCR2 and not in CCR5 for the inhibition effect of TAK-779. Interestingly, comparison of this binding site to the known ZM241385 (antagonist) binding site in human adenosine A2A receptor crystal structure (Jakkola et al 2008), shows that the residue corresponding to the position 3.33 is L85^{3.33} in the human A2A receptor, and shows strong van der Waals contact with the aromatic ring system in ZM241385. Positions 3.36 and 6.48 in CCR2 seem to be important for the expression of the receptor and may be related to the inter-helical interactions. Position 6.55 is critical in subtype selectivity, since it shows substantial effect on antagonist inhibition in CCR2 for both TAK-779 and Teijin compound 1 and has no effect on TAK-779 in CCR5 for HIV viral entry (Dragic et al 2000). This position 6.55 is also critical to differentiating two different antagonists for the same receptor. For example, mutation of I259A^{6.55} in CCR1 leads to substantial lowering of inhibition for BX471 (Vaidehi et al 2006) and not for UCB35625 (de Mendonca et al 2005). It is noteworthy that the corresponding residue in

A2A crystal structure, N253^{6.55} makes two hydrogen bonds with the bicyclic triazolotriazine ring system in ZM241385 and this could contribute to the subtype specificity of ZM241385 (Jakkola et al 2008). E7.39 is an important residue for agonist and antagonist activity in all the four chemokine receptors, CCR1, CCR2, CCR3 and CCR5. This position is Ile274^{7.39} in A2A, and makes a weak hydrophobic interaction in the A2A crystal structure. We have compared the binding site of antagonists in the chemokine receptors only to the A2A crystal structure due to the similarities in the nature of the antagonists studied here and ZM241385.

Conclusions: Using a combination of computational predictions followed by site directed mutagenesis, radiolabeled binding and chemotaxis experiments, we observe that the structurally distinct Teijin and TAK-779 antagonists bind in slightly different but overlapping intrahelical transmembrane pockets in CCR2. A group of five conserved residues, W98^{2.60}, H121^{3.33}, I263^{6.55}, E291^{7.39} and T292^{7.40} play a critical role in the activity of Teijin compound 1 at CCR2, while only W98^{2.60} and T292^{7.40} of this group play an important role in TAK-779 activity. Mutation of W86^{2.60} and Y108^{3.32} significantly affects the activity of TAK-779 at CCR5. We also observed that mutation of Y49A^{1.39}, W98A^{2.60}, Y120A^{3.32}, and E291Q^{7.39} of CCR2 severely reduced the affinity of the receptor for CCL2. We hypothesize that these residues are involved in a network of inter-helical interactions, and disruption of the network leads to reduced binding and potency efficacy of the agonist CCL2. E291^{7.39} of CCR2 and E283^{7.39} in CCR5 play an important role in mediating receptor conformations stabilized by either antagonist, leading to an ensemble of receptor conformations.

In this work, we have demonstrated an iterative process between computational predictions and experimental validation, where the experimental results were subsequently used

MOL# 53470

to reexamine and refine the docked conformations of TAK-779 in CCR2. The effective process of computationally predicting testable hypotheses has led to not only a reduction of the number of experiments, but also to valuable insights into the role of E291^{7,39} in mediating the conformational flexibility of the CCR2 and CCR5 receptors. Based on the results, we hypothesize that a receptor activation network located between TM 1, 2 and 7 and consisting of the highly conserved residues Y49^{1,39}, W98^{2,60}, Y120^{3,32}, E291^{7,39} is either stabilized in an active state by the agonist or disrupted by an antagonist. It should be noted that these residues are not strictly conserved across all the CC chemokine receptors, suggesting that a “one size fits all” model of chemokine receptor activation/antagonism will not be forthcoming.

References

- Allen, S.J., Crown S.E., and Handel, T.M., (2007), Chemokine: Receptor, Structure, Interactions and Antagonism, *Ann. Rev. Immunol.* **25**, 787-820.
- Baba, M., Kanzaki, N., Okamoto, M., Sawada, H., Iizawa, Y., Shiraishi, M., Aramaki, Y., Okonogi,., Nishimura, O.K., Ogawa, Y., Meguro, K., and Fujino, M. (1999) A small-molecule, nonpeptide CCR5 antagonist with highly potent and selective anti-HIV-1 activity, *Proc Natl Acad Sci U S A* **96**, 5698-5703.
- Ballesteros J, Weinstein H (1995) Integrated methods for modeling G-protein coupled receptors. *Methods Neurosci* **25**, 366–428.
- Berkhout T.A., Blaney F.E., Bridges A.M., Cooper D.G, Forbes I.T., Gribble, A.D., Groot, P.H.E., Hardy,A., Ife, R.J., Kaur,R., Moores, K.E., Shillito,H., Willetts, J., and Witherington, J., (2003) CCR2: characterization of the antagonist binding site from a combined receptor modeling/mutagenesis approach. *J. Med. Chem.* **46**, 4070–86.
- Bhattacharya S., Hall, S.E., and Vaidehi, N. (2008), Agonist-induced conformational changes in bovine rhodopsin: insight into activation of G-protein-coupled receptors, *J. Mol. Biol.* **382**, 539-555.
- Charo, I. F., Myers, S. J., Herman, A., Franci, C., Connolly, A. J., and Coughlin, S. R. (1994), Molecular cloning and functional expression of two monocyte chemoattractant protein 1 receptors reveals alternative splicing of the carboxyl-terminal tails, *Proc Natl Acad Sci USA* **91**, 2752-2756.
- Charo, I. F., and Ransohoff, R. M. (2006), The many roles of chemokines and chemokine receptors in inflammation, *N Engl J Med* **354**, 610-621.
- Cherezov V, Rosenbaum DM, Hanson MA, Rasmussen SG, Thian FS, Kobilka TS, Choi HJ, Kuhn P, Weis WI, Kobilka BK, Stevens RC. (2007), High-resolution crystal structure of an engineered human beta2-adrenergic G protein-coupled receptor. *Science*, **318**, 1258-65.
- Daugherty B.L., Siciliano S.J., and Springer M.S. (2000), Radiolabeled chemokine binding assays. *Methods MolBiol.* **138**, 129-134.
- de Mendonça FL, da Fonseca PC, Phillips RM, Saldanha JW, Williams TJ, Pease JE. (2005), Site-directed mutagenesis of CC chemokine receptor 1 reveals the mechanism of action of UCB 35625, a small molecule chemokine receptor antagonist, *J Biol Chem.* **280**, 4808-16.
- Doms, R. W., and Peiper, S. C. (1997), Unwelcomed guests with master keys: how HIV uses chemokine receptors for cellular entry, *Virology* **235**, 179-190.

Dragic, T., Trkola, A., Thompson, D.A., Cormier, E.G., Kajumo, F.A., Maxwell, E., Lin, S.W., Ying, W., Smith S.O., Sakmar, T.P., and Moore J.P., (2000), A binding pocket for a small molecule inhibitor of HIV-1 entry within the transmembrane helices of CCR5, *Proc. Natl. Acad. Sci USA*, **97**, 5639-5644.

Frantz, S. (2005), Drug discovery: playing dirty, *Nature* **437**, 942-943.

Gallivan J.P., and Dougherty D.A., (1999), Cation-pi interactions in structural biology, *Proc Natl Acad Sci U S A*. **96**, 9459-9464.

Ghosh, A., Rapp, C.S., and Friesner, R.A., (1998), Generalized Born model based on a surface integral formulation. *J.Phys. Chem B* **102**, 10983-10990.

Gong JH, Clark-Lewis I. (1995), Antagonists of monocyte chemoattractant protein 1 identified by modification of functionally critical NH2-terminal residues. *J. Exp. Med.* **181**:631–640.

Govaerts, C., Bondue, A., Springael J., Olivella M., Deupi, X., Le Poul, E., Wodak S.J., Parmentier, M., Pardo, L., and Blanpain C. (2003), Activation of CCR5 by Chemokines Involves an Aromatic Cluster between Transmembrane Helices 2 and 3, *J. Biol. Chem.*, **278**, 1892-1903.

Hall S.E., (2005), Development of structure prediction methods for G-protein coupled receptors - Ph.D. Thesis, California Institute of Technology.

Heo, J., Vaidehi, N., Wendel J., and Goddard W.A., (2007), Prediction of the 3D structure of rat MrgA GPCR and identification of its binding site, *J. Mol. Graph. Model.* **26**, 800-812.

Jaakola VP, Griffith MT, Hanson MA, Cherezov V, Chien EY, Lane JR, Ijzerman AP, Stevens RC. (2008), The 2.6 angstrom crystal structure of a human A2A adenosine receptor bound to an antagonist, *Science*, **322**, 1211-1217.

Jarnagin K, Grunberger D, Mulkins M, Wong B, Hemmerich S, Paavola C, Bloom A, Bhakta S, Diehl F, Freedman R, McCarley D, Polsky I, Ping-Tsou A, Kosaka A, Handel TM (1999), Identification of surface residues of the monocyte chemotactic protein 1 that affect signaling through the receptor CCR2. *Biochemistry* **38**:16167–16177.

Lieberman-Blum S.S., Fung H.B., Bandres J.C., (2008), Maraviroc: a CCR5-receptor antagonist for the treatment of HIV-1 infection, *Clin Ther.*, **30**, 1228-50.

Maeda K, Das D, Ogata-Aoki H, Nakata H, Miyakawa T, Tojo Y, Norman R, Takaoka Y, Ding J, Arnold GF, Arnold E, Mitsuya H., (2006), Structural and molecular interactions of CCR5 inhibitors with CCR5, *J. Biol. Chem.*, 281, 12688-98.

Mirzadegan T, Diehl F, Ebi B, Bhakta S, Polsky I, McCarley D, Mulkins M, Weatherhead GS, Lapierre JM, Dankwardt J, Morgans D Jr, Wilhelm R, Jarnagin K. (2000) Identification of the binding site for a novel class of CCR2b chemokine receptor antagonists—binding to a common chemokine receptor motif within the helical bundle. *J. Biol. Chem.* **275**, 25562–25571.

Moree, W. J., Kataoka, K., Ramirez-Weinhouse, M. M., Shiota, T., Imai, M., Tsutsumi, T., Sudo, M., Endo, N., Muroga, Y., Hada, T., Fanning, D., Saunders, J., Kato, Y., Myers, P. L., and Tarby, C. M. (2008), Potent antagonists of the CCR2b receptor. Part 3: SAR of the (R)-3-aminopyrrolidine series *Bioorg Med Chem Lett* **18**, 1869-1873.

Morphy, R., and Rankovic, Z. (2005) Designed multiple ligands. An emerging drug discovery paradigm., *J Med Chem* **48**, 6523-6543.

Murphy, P. M. (1994) The molecular biology of leukocyte chemoattractant receptors, *Annu Rev Immunol* **12**, 593-633.

Palczewski K, Kumasaka T, Hori T, Behnke CA, Motoshima H, Fox BA, Le Trong I, Teller D.C., Okada T, Stenkamp R.E., Yamamoto M., Miyano M., **2000**, Crystal structure of rhodopsin: A G protein-coupled receptor, *Science*, 289, 739-745.

Ribeiro, S., and Horuk, R. (2005) *Chemokine receptor antagonists from the bench to the clinic*, Wiley-VCH, Weinheim.

Samson, M., Labbe, O., Mollereau, C., Vassart, G., and Parmentier, M. (1996) Molecular cloning and functional expression of a new human CC-chemokine receptor gene, *Biochemistry* **35**, 3362-3367.

Schertler, G.F.X. (1998), Structure of rhodopsin. *Eye* **12**, 504-510.

Seibert, C., Ying, W., Gavrilov, S., Tsamis, F., Kuhmann, S.E., Palani, A., Tagat, J.R., Clader, J.W., McCombie, S.W., Baroudy, B.M., Smith, S.O., Dragic, T., Moore, J.P., and Sakmar, T.P., (2006), Interaction of small molecule inhibitors of HIV-1 entry with CCR5, *Virology*, **349**, 41-54.

Seto, M., Aikawa, K., Miyamoto, N., Aramaki, Y., Kanzaki, N., Takashima, K., Kuze, Y., Iizawa, Y., Baba, M., and Shiraishi, M. (2006) Highly potent and orally active CCR5 antagonists as anti-HIV-1 agents: synthesis and biological activities of 1-benzazocine derivatives containing a sulfoxide moiety, *J Med Chem* **49**, 2037-2048.

Stroke, I. L., Cole, A. G., Simhadri, S., Brescia, M. R., Desai, M., Zhang, J. J., Merritt, J. R., Appell, K. C., Henderson, I., and Webb, M. L. (2006), Identification of CXCR3 receptor agonists in combinatorial small-molecule libraries, *Biochem Biophys Res Commun* **349**, 221-228.
Szekanecz, Z., Szucs, G., Szanto, S., and Koch, A. E. (2006) Chemokines in rheumatic diseases, *Curr Drug Targets* **7**, 91-102.

Trabanino, R., Hall, S.E., Vaidehi, N., Floriano, W., Goddard, W.A. (2004) First Principles Prediction of the structure and Function of G protein-coupled receptors: validation for bovine rhodopsin *Biophys. J.*, **86**, 1904-1921.

MOL# 53470

Vaidehi, N., Schlyer, S., Trabanino, R. J., Floriano, W. B., Abrol, R., Sharma, S., Kochanny, M., Koovakat, S., Dunning, L., Liang, M., Fox, J. M., de Mendonca, F. L., Pease, J. E., Goddard, W. A., 3rd, and Horuk, R. (2006) Predictions of CCR1 chemokine receptor structure and BX 471 antagonist binding followed by experimental validation, *J Biol Chem* **281**, 27613-27620.

Vriend, G. (1990) WHAT IF—a molecular modeling and drug design program. *J. Mol. Graph.* **8**, 52–56.

Wise EL, Duchesnes C, da Fonseca PC, Allen RA, Williams TJ, Pease JE. (2007), Small molecule receptor agonists and antagonists of CCR3 provide insight into mechanisms of chemokine receptor activation, *J. Biol. Chem.*, 282, 27935-43.

Zhang Y, Rollins BJ. (1995), A dominant negative inhibitor indicates that monocyte chemoattractant protein 1 functions as a dimer, *Mol. Cell. Biol.* **15**, 4851–4855.

[‡] Both these authors contributed equally to the work.

MOL# 53470

This work was funded by Berlex BioSciences (Grant number RCON5924) and an award from the Arthritis Research Campaign (Grant number 18303).

Figure Legends

Figure 1 Chemical structures of the CCR2 and CCR5 dual antagonist TAK-779 and the CCR2 specific antagonist Teijin compound 1. The reported IC_{50} for TAK-779 binding to CCR5 is 1 nM and to CCR2 is 27 nM (Baba et al 1999). The reported binding affinity of the Teijin compound 1 to CCR2 is 180 nM (Moree et al 2008).

Figure 2: **A.** Apo-protein structural model of CCR2, one from the ensemble of structural models, showing the hydrogen bond network between D88^{2.50} and N60^{1.50}, and N301^{7.49}. Another inter-helical hydrogen bond is between W165^{4.50} and N83^{2.45}. **B:** The CCR5 apo-protein structural model showing hydrogen bond network between N48^{1.50} and D76^{2.50} and N293^{7.49}. Also the shown is the hydrogen bond between W153^{4.50} and N71^{2.45}. These hydrogen bonds are observed in class A GPCR crystal structures available so far.

Figure 3 The predicted structure of human CCR2 with antagonist binding sites (A) Side view of the binding site of Teijin compound 1 (green) and TAK-779 (cyan) with the extracellular region at the top (B) Top view of the predicted binding sites of TAK-779 and Teijin compound 1 in the CCR2 binding pocket. (C) Residues within 5Å in the binding site of Teijin compound 1. (D) Residues within 5Å of the binding site of TAK-779 in CCR2. Dashed lines indicate residues contributing 1 to 5 kcal/mol to the ligand interaction energy.

Figure 4 Receptor expression and inhibition of CCL2-mediated chemotaxis of CCR2 mutants by the antagonists. (A) Cell surface expression of CCR2 point mutants. Each of the HA-tagged CCR2 point mutant constructs was transiently transfected independently into L1.2 cells as

previously described (Vaidehi et al 2006). Twenty-four hours after transfection, cells were incubated with anti-HA antibody and cell surface expression was analyzed by flow cytometry, following subtraction of irrelevant staining with an isotype control. Surface expression is shown as a percentage of the expression observed for cells simultaneously transfected with the WT CCR2 construct. Data is the mean \pm S.E of at least three experiments. **(B)** Chemotaxis of CCR2 transfectants to increasing concentrations of CCL2. Data is shown as the chemotactic index and represents the mean \pm S.E. from 3 separate experiments; **(C and D)** Chemotaxis of transfectants expressing WT CCR2 or selected CCR2 point mutants to a fixed concentration of 1nM CCL2 in the presence of increasing concentrations of Teijin compound 1 (Panel C) or TAK-779 (Panel D). The data shown is the mean \pm S.E. of 3 separate experiments. **(E and F)** Chemotaxis of transfectants expressing WT CCR2 or selected CCR2 point mutants to a fixed concentration of 1 nM CCL2 (WT CCR2), 10nM CCL2 (W86A and Y120A mutants) and 100nM CCL2 (E291Q mutant) in the presence of increasing concentrations of Teijin compound 1 (Panel E) or TAK-779 (Panel F). The data shown is the mean mean \pm S.E. of 3 separate experiments.

Figure 5 The predicted structure of human CCR5 with TAK-779 bound. (A): Side view of the binding site of TAK-779 (shown in pink) in CCR5 with the extracellular region at the top. (B) Top view of the predicted binding site of TAK-779 in CCR5. (C) Details of the predicted binding site showing all residues within 5Å for TAK-779 in CCR5.

Figure 6 Receptor expression and CCL3-mediated chemotaxis of CCR5 mutants. (A). Cell surface expression of CCR5 mutants relative to that of WT CCR5. Data represents the mean \pm S.E. from 8 separate experiments *** denote p values of <0.001 and 0.05 respectively,

MOL# 53470

compared to WT CCR5 expression as deduced by 2-way ANOVA and Bonferroni's multiple comparisons test. (B) Chemotaxis of CCR5 transfectants to increasing concentrations of CCL3. Data is shown as the chemotactic index and represents the mean \pm S.E. from 3 separate experiments *** denotes a p value of <0.001 compared to WT CCR5 transfectants as deduced by 2-way ANOVA and Bonferroni's multiple comparisons test. (C) Chemotaxis of transfectants expressing WT CCR5 or selected CCR5 point mutants to a fixed concentration of 30 nM CCL3 in the presence of increasing concentrations of TAK-779. The data shown is the mean of 3-5 separate experiments \pm . S.E.

Table 1: A summary of data from chemotaxis assays in Figures 4C to 4F where the migration of cells expressing WT CCR2 or selected CCR2 point mutants to concentrations of CCL2 (shown in parenthesis next to the mutant name) was inhibited by increasing concentrations of TAK-779 or Teijin compound 1. The data is representative of 3 experiments. NOA represents “no observable antagonism” where at a 1000-fold excess or greater of antagonist, less than 50% inhibition of migration was observed. S.E. represents the standard error.

Construct	Antagonist			
	TAK-779		Teijin compound 1	
	IC ₅₀ (nM)	Log IC ₅₀ [M] ± S.E.	IC ₅₀ (nM)	Log IC ₅₀ [M] ± S.E.
WT CCR2 (1nM)	5.78	-8.24 ± 0.20	370.68	-6.43 ± 0.17
W98A ^{2.60} (10nM)	142.23	-6.85 ± 0.33	13995.87	-4.85 ± 39.64
Y120A ^{3.32} (10nM)	2.29	-8.64 ± 0.08	3.92	-8.41 ± 0.19
H121A ^{3.33} (1nM)	7.42	-8.13 ± 0.21	20276.82	-4.69 ± 2.70
F125A ^{3.37} (1nM)	7.80	-8.11 ± 0.18	152.26	-6.81 ± 0.11
I208A ^{5.44} (1nM)	4.87	-8.31 ± 0.15	332.66	-6.48 ± 0.10
I263A ^{6.55} (1nM)	6.26	-8.20 ± 0.15	4808.39	-5.32 ± 0.36
E291Q ^{7.39} (100nM)	0.69	-9.16 ± 0.04	26.79	-7.57 ± 0.25
T292V ^{7.40} (1nM)	414.70	-6.38 ± 1.15	NOA	NOA

Table 2: A summary of data from competitive binding experiments. Displacement of ^{125}I -CCL2 from cells expressing WT CCR2 and selected CCR2 point mutants, with increasing concentrations of unlabelled CCL2, TAK-779 or Teijin compound 1. The data is representative of 3 experiments. NSB represents “no specific binding”, where at a 1000-fold excess of unlabelled CCL2, less than 50% displacement of ^{125}I -CCL2 was observed. NOD represents “no observable displacement” where at a 1000-fold excess or greater of antagonist, less than 50% displacement of ^{125}I -CCL2 was observed. S.E. represents the standard error.

Construct	CCL2 displacement		TAK-779 displacement		Teijin compound 1 displacement	
	IC ₅₀ (nM)	Log IC ₅₀ [M] ± S.E.	IC ₅₀ (nM)	Log IC ₅₀ [M] ± S.E.	IC ₅₀ (nM)	Log IC ₅₀ [M] ± S.E.
WT CCR2	9.60	-8.02±0.07	49.30	-7.307 ± 0.39	405.51	-6.392 ±0.09
Y49A ^{1.39}	NSB	NSB	NSB	NSB	NSB	NSB
W98A ^{2.60}	NSB	NSB	NSB	NSB	NSB	NSB
Y120A ^{3.32}	NSB	NSB	NSB	NSB	NSB	NSB
H121A ^{3.33}	4.18	-8.38±0.03	19.90	-7.70 ± 0.04	1127.20	-5.948 ± 0.43
I263A ^{6.55}	3.18	-8.50±0.04	12.85	-7.89 ± 0.03	787.05	-6.104 ±0.13
E291Q ^{7.39}	NSB	NSB	NSB	NSB	NSB	NSB
T292V ^{7.40}	9.18	-8.04±0.12	663.74	-6.178 ± 9.34	NOD	NOD

Table 3: A summary of data from chemotaxis assays in Figures 6C, where the migration of cells expressing WT CCR5 or selected CCR5 point mutants to a fixed concentration of 30 nM CCL3 was inhibited by increasing concentrations of TAK-779. The data is representative of 3-5 experiments. S.E. represents the standard error.

Construct	TAK-779	
	IC₅₀ (nM)	Log IC₅₀ [M] ± S.E.
WT CCR5	1.86	- 8.73 ± 0.11
W86A ^{2.60}	229.09	-6.64 ± 0.20
Y108A ^{3.32}	331.13	-6.48 ± 0.22
F109A ^{3.33}	6.61	- 8.18 ± 0.11
E283Q ^{7.39}	16.22	-7.79 ± 0.22

MOL# 53470

Table 4: A summary of data from competitive binding experiments. Displacement of ¹²⁵I-CCL3 from cells expressing WT CCR5 and selected CCR5 point mutants, with increasing concentrations of unlabelled CCL3 or TAK-779. The data is representative of 3-4 experiments. NOD represents “no observable displacement” where at a 1000-fold excess of unlabelled ligand, less than 50% displacement of ¹²⁵I-CCL3 was observed.

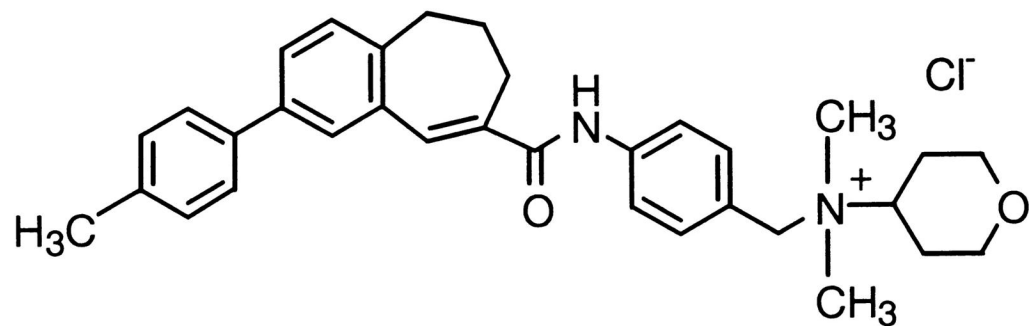
Construct	Competing Ligand			
	CCL3		TAK-779	
	IC ₅₀ (nM)	Log IC ₅₀ [M] ± S.E.M.	IC ₅₀ (nM)	Log IC ₅₀ [M] ± S.E.M.
WT CCR5	28.12	-7.55 ± 0.16	7.12	-8.15 ± 0.10
W86A ^{2.60}	32.26	-7.51 ± 0.29	NOD	NOD
Y108A ^{3.32}	29.51	-7.53 ± 0.51	NOD	NOD
F109A ^{3.33}	12.44	-7.91 ± 0.24	14.45	-7.84 ± 0.19
E283Q ^{7.39}	52.84	-7.28 ± 0.56	11.59	-7.94 ± 0.16

Table 5: Summary of the mutation results and its effect on inhibition by Teijin compound and TAK-779 in CCR2 and CCR5. The results compiled here are from this study only. “↑” means higher than wild type (WT). “↓” signifies lower than WT receptor; “NA” is not available or performed in this study. “NG” is negligible effect; “WT” means same level of effect as in the wild type receptor.

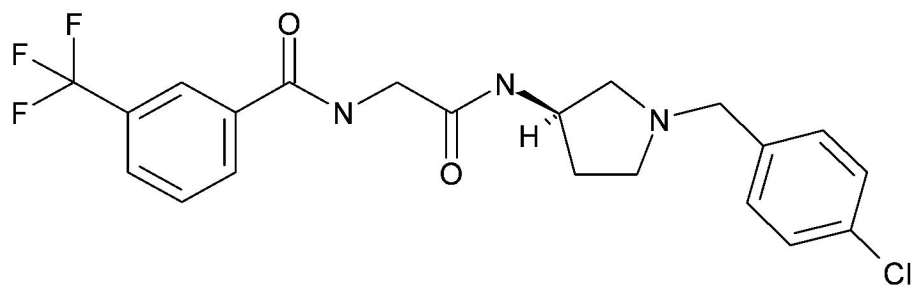
Mutants		Expression level		Chemotaxis activity		Teijin Compound 1 in CCR2	TAK-779 in CCR2	TAK-779 in CCR5
CCR2	CCR5	CCR2	CCR5	CCR2	CCR5			
Y49A ^{1.39}	Y37A ^{1.39}	↑	↑	Nil	Nil	Nil	Nil	Nil
W98A ^{2.60}	W86A ^{2.60}	↓	↑	↓	WT	↑	↑	↑
F116A ^{3.28}	NA	Nil	NA	Nil	NA	Nil	Nil	NA
Y120A ^{3.32}	Y108A ^{3.32}	↑	↑	↓	WT	↓	↓	↑
H121A ^{3.33}	F109A ^{3.33}	WT	↑	WT	WT	↑	↓	↓
Y124A ^{3.36}	NA	Nil	NA	Nil	NA	Nil	Nil	NA
F125A ^{3.37}	NA	↑	NA	WT	NA	NG	NG	NA
I208A ^{5.44}	NA	WT	NA	↑	NA	NG	NG	NA
W256A ^{6.48}	NA	Nil	NA	Nil	NA	Nil	Nil	NA
I263A ^{6.55}	NA	↓	NA	↑	NA	↑	↓	NA
E291A ^{7.39}	NA	↑	NA	Nil	NA	NA	NA	NA
E291Q ^{7.39}	E283Q ^{7.39}	WT	↑	↓	↓	↑	↓	↓
T292V ^{7.40}	NA	WT	NA	↑	NA	↑	↑	NA

Table 6: List of conserved residues in four chemokine receptors that have been mutated to alanine in this and other published studies (Mirzadegan et al 2000, Dragic et al 2000, Berkhout et al 2003, de Mendonca et al 2005, Seibert et al 2006, Maeda et al 2006 and Wise et al 2007). Mutation of the residues underlined and in bold font has been reported to display a loss of antagonist activity. Residues in grey color have no significant effect on either agonist or antagonist activity; residues in *italics* indicate mutants with poor cell surface expression and /or reduced chemotactic activity compared to wild type receptor; residues in black color normal font have not been mutated; residues in *italics* and underlined have significant effect on small molecule agonist activity. E7.39 mutation results are for E7.39Q mutation and not the alanine mutation.

CCR1	CCR2	CCR3	CCR5
<u>Y41</u> ^{1.39}	<i>Y49</i> ^{1.39}	<u><i>Y41</i></u> ^{1.39}	<u>Y37</u> ^{1.39}
W90 ^{2.60}	<u>W98</u> ^{2.60}	W86 ^{2.60}	<u>W86</u> ^{2.60}
<u>Y113</u> ^{3.32}	<u>Y120</u> ^{3.32}	<u>Y113</u> ^{3.32}	<u>Y108</u> ^{3.32}
<u>Y114</u> ^{3.33}	<u>H121</u> ^{3.33}	H114 ^{3.33}	F109 ^{3.33}
L117 ^{3.36}	<i>Y124</i> ^{3.36}	L117 ^{3.36}	Y112 ^{3.36}
W252 ^{6.48}	<i>W256</i> ^{6.48}	W252 ^{6.48}	W248 ^{6.48}
<u>I259</u> ^{6.55}	<u>I263</u> ^{6.55}	I259 ^{6.55}	L255 ^{6.55}
<u>E287</u> ^{7.39}	<u>E291</u> ^{7.39}	<u>E287</u> ^{7.39}	<u>E283</u> ^{7.39}
V288 ^{7.39}	<u>T292</u> ^{7.40}	V288 ^{7.39}	T284 ^{7.40}



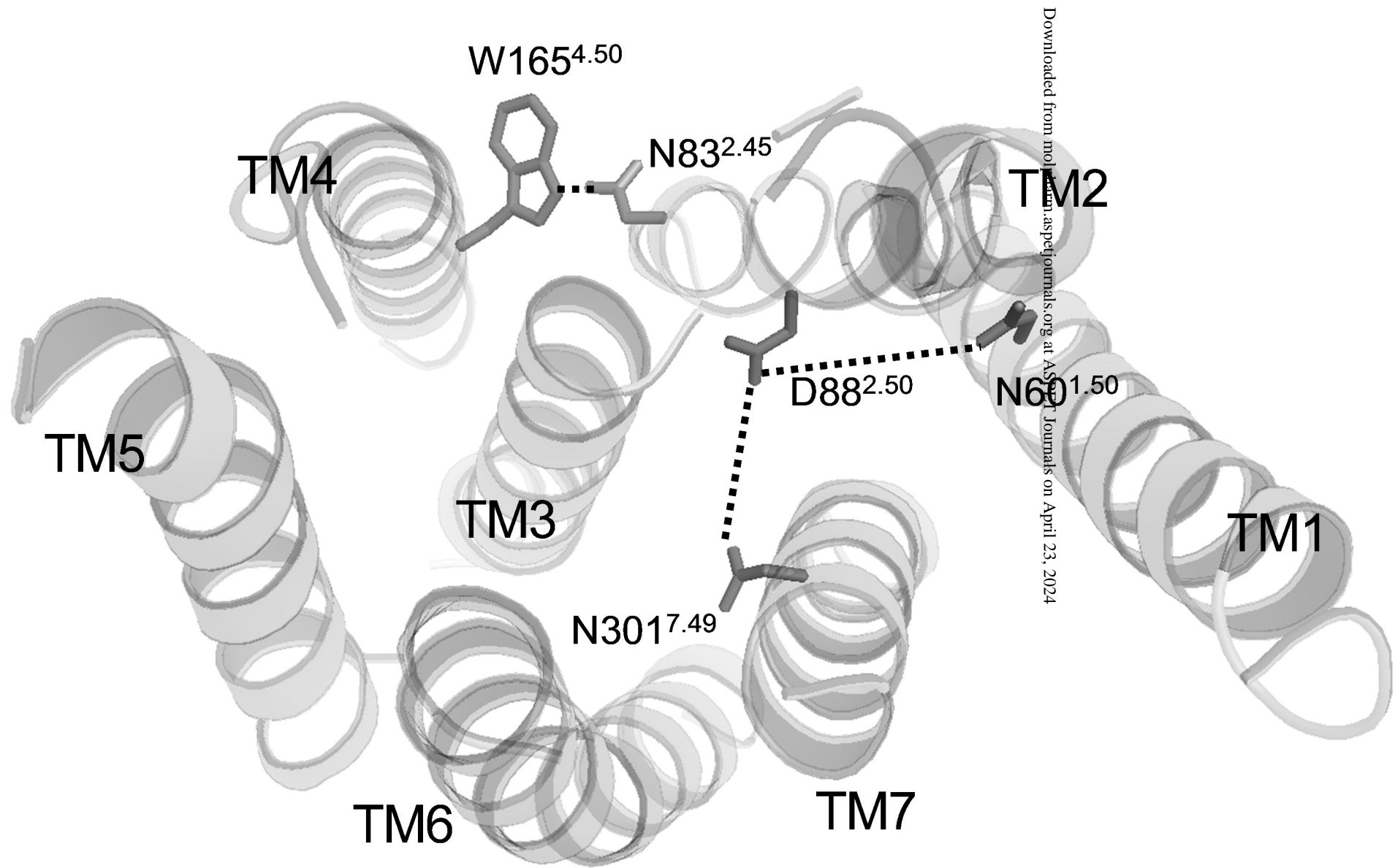
TAK 779



Teijin compound 1

Figure 1

Figure 2A



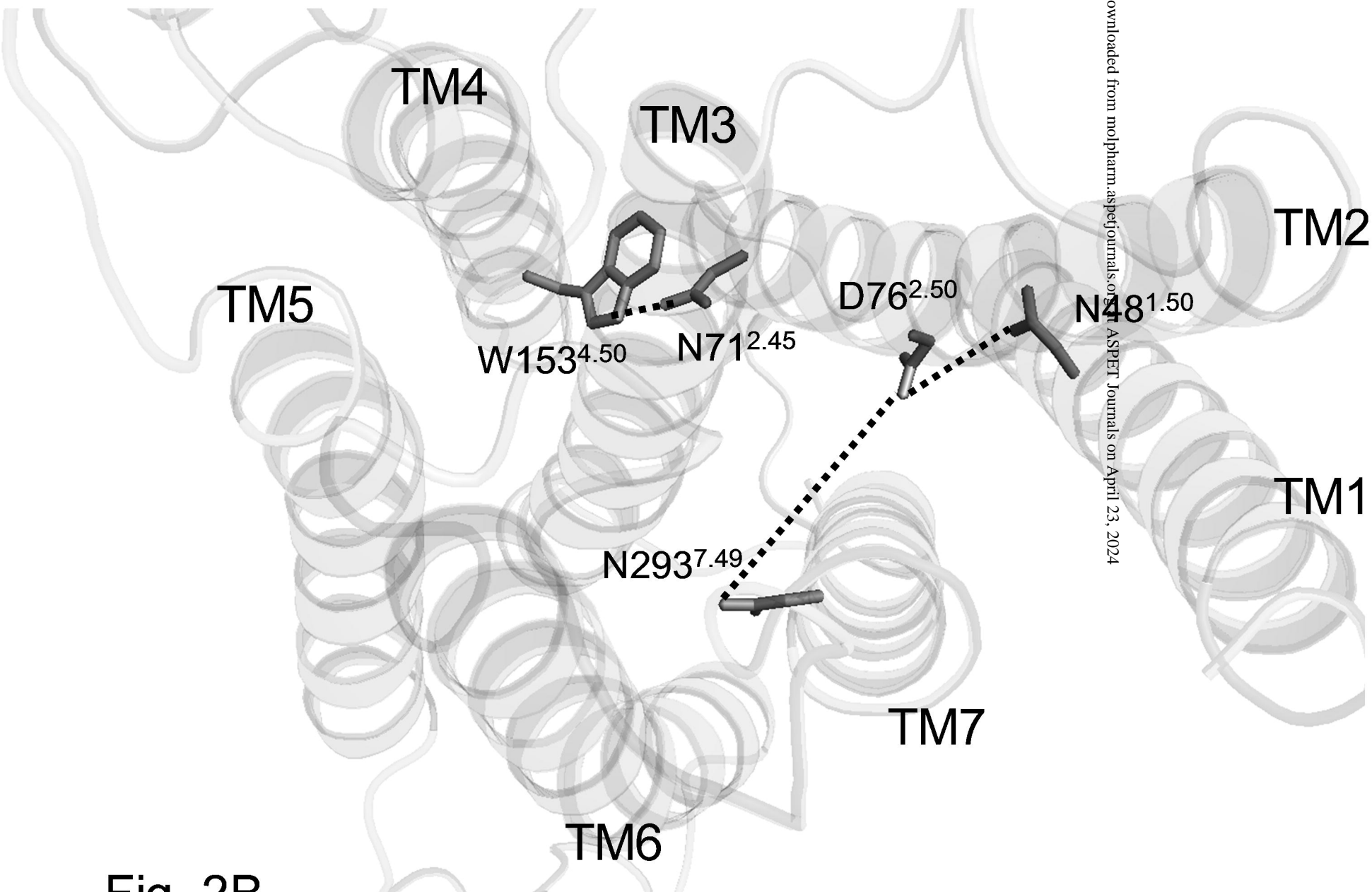


Fig. 2B

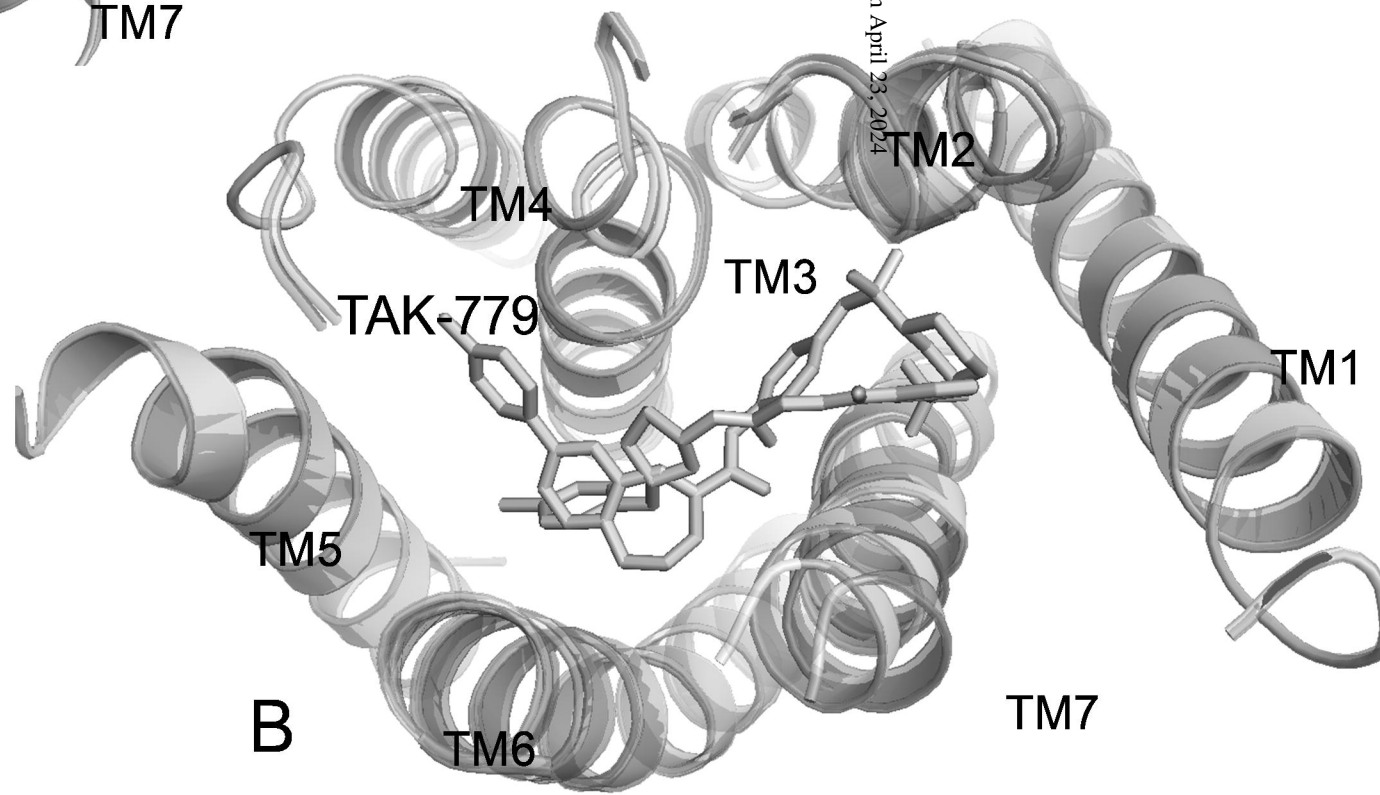
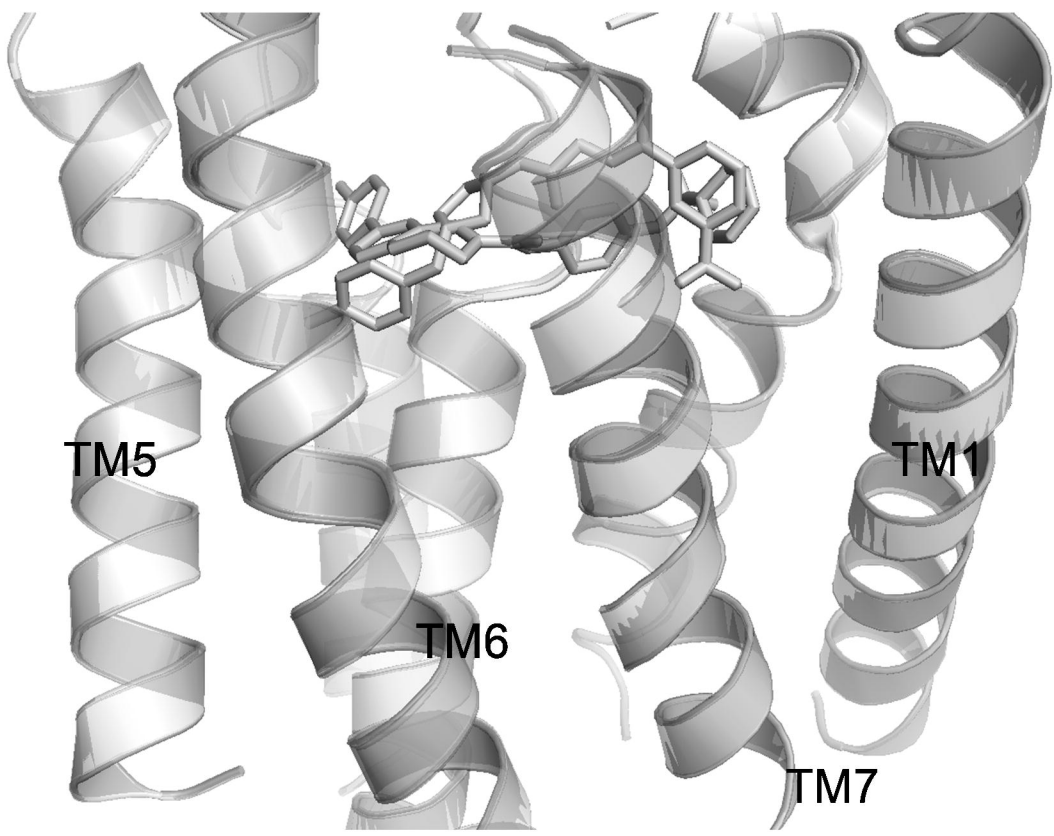
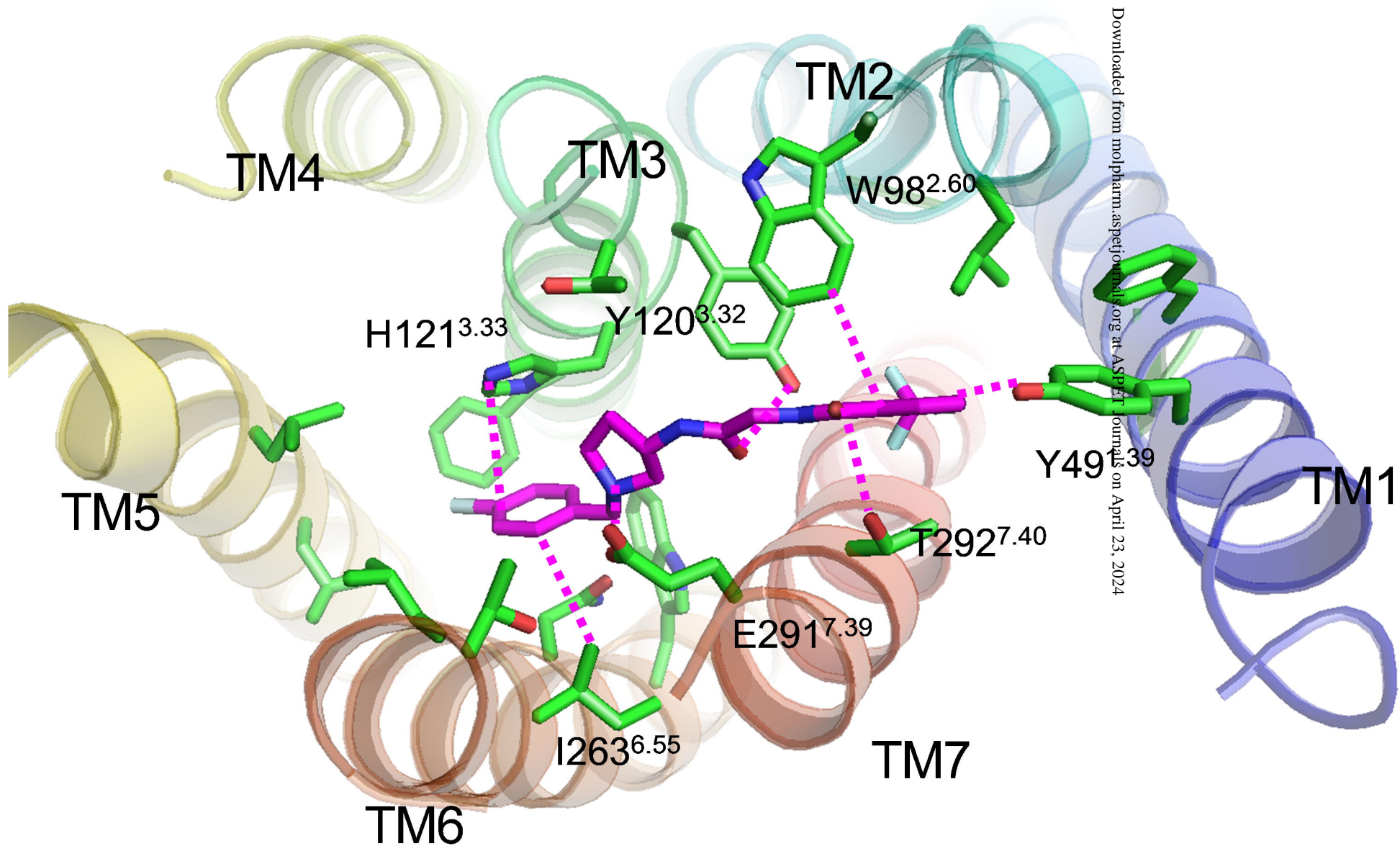


Figure 3



Downloaded from molpharm.aspetonline.org at ASPET Journals on April 23, 2024

Figure 3 C

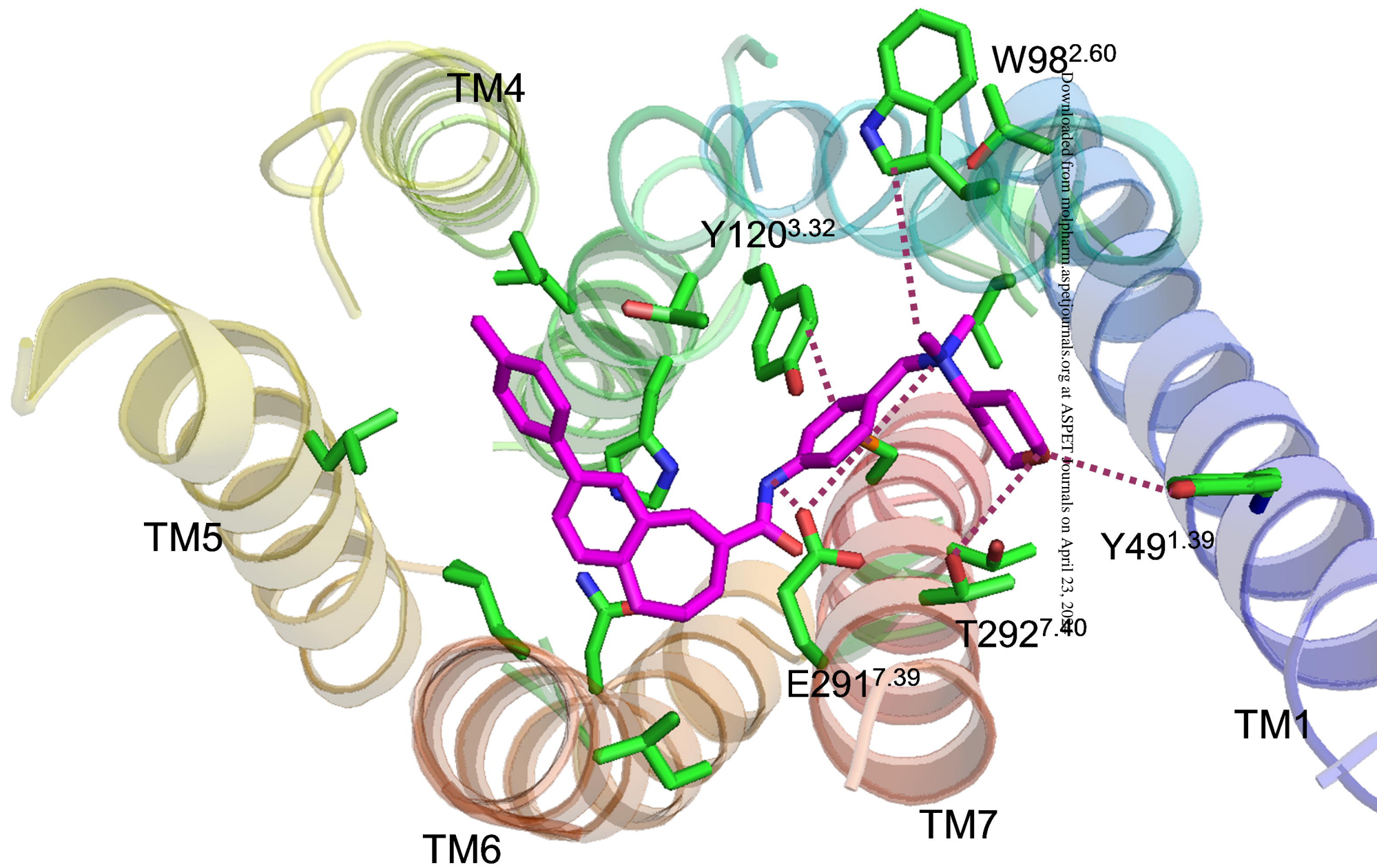
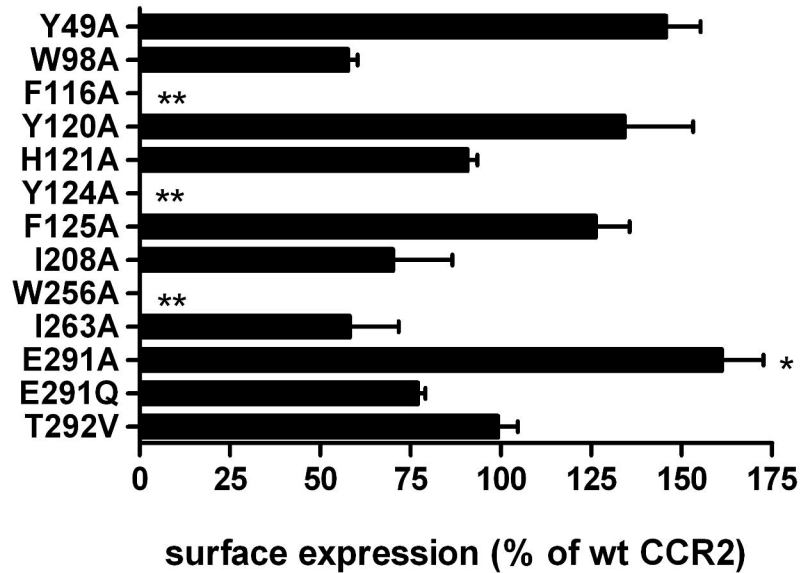
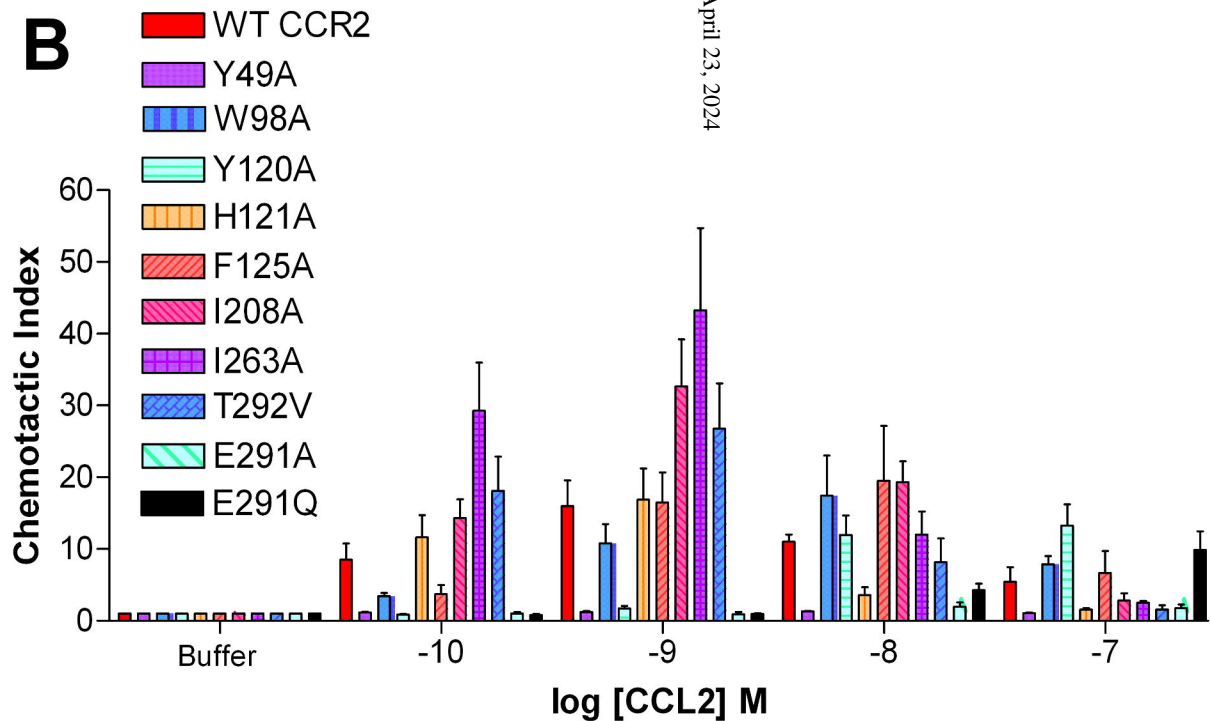
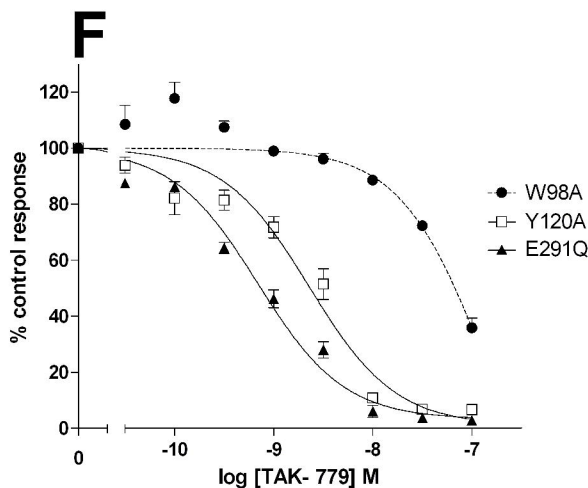
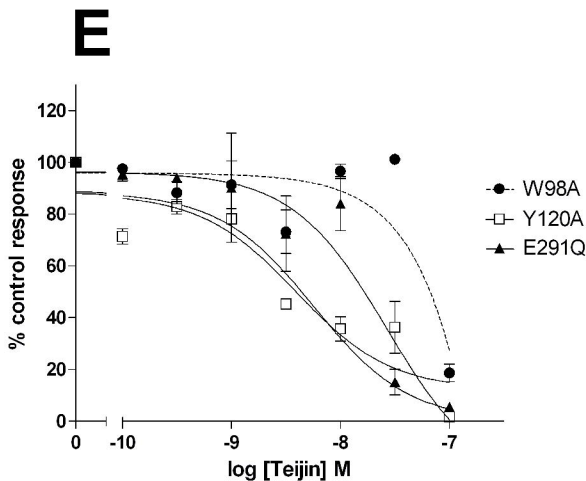
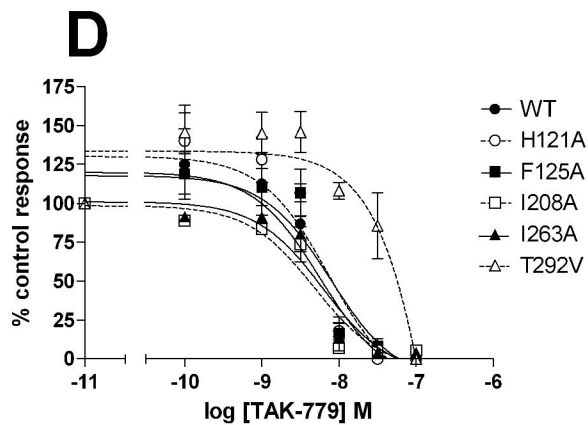
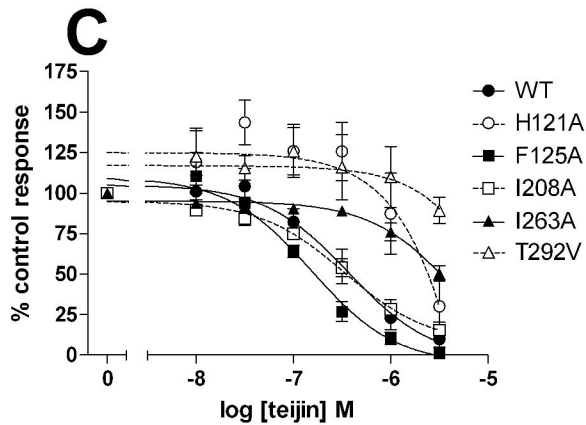
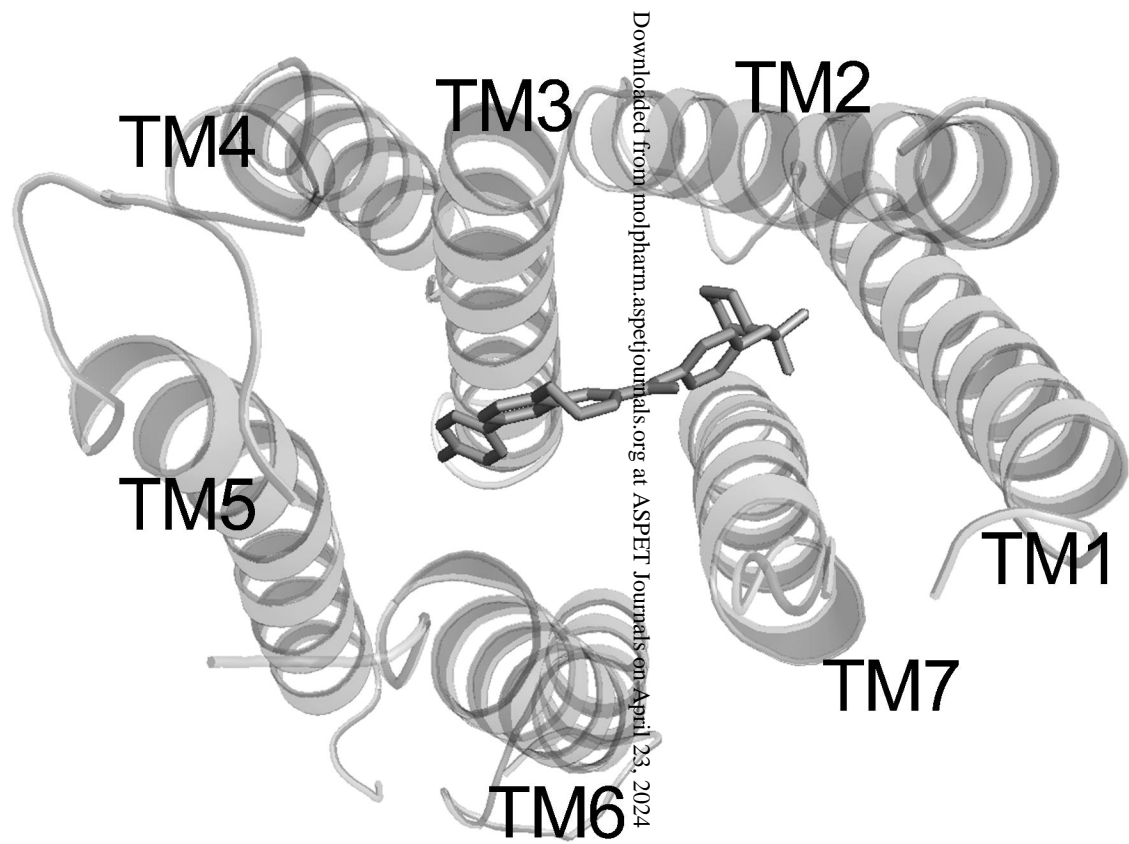
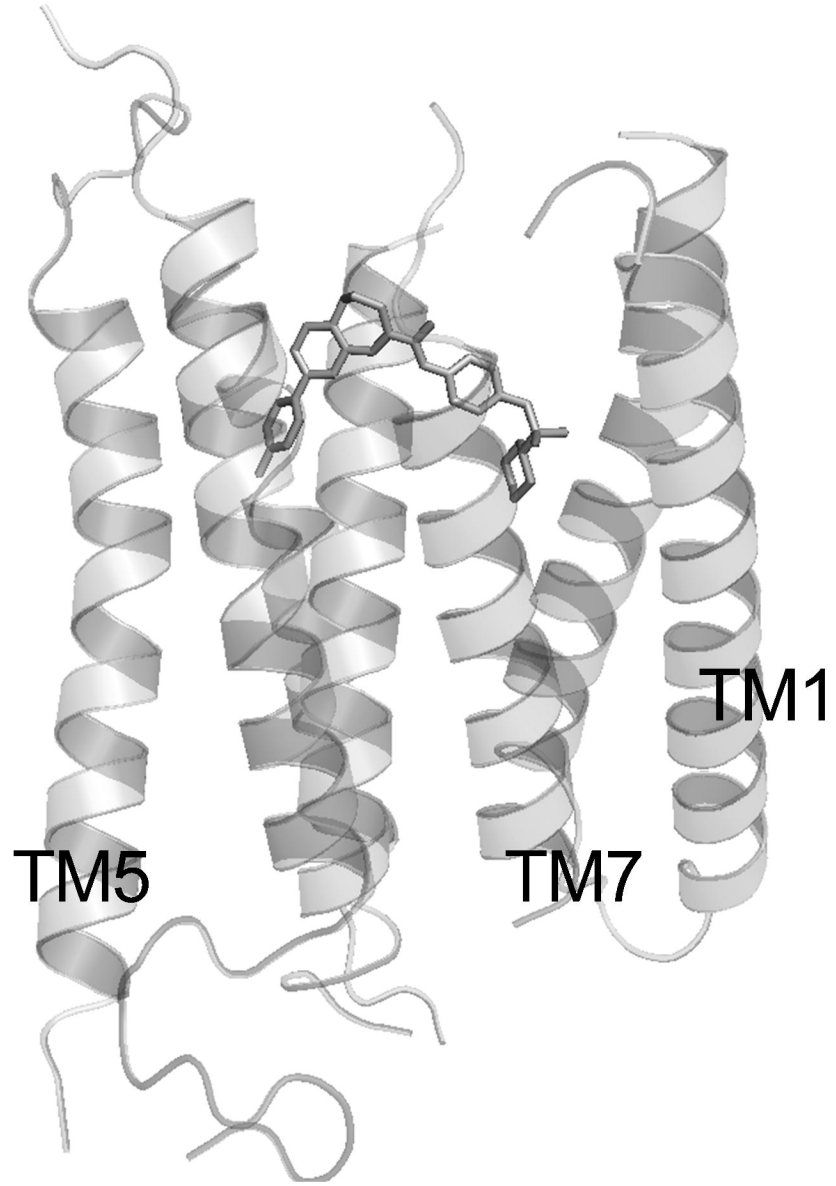


Figure 3 D

A**B**





Downloaded from molpharm.aspetjournals.org at ASPET Journals on April 23, 2024

Figure 5

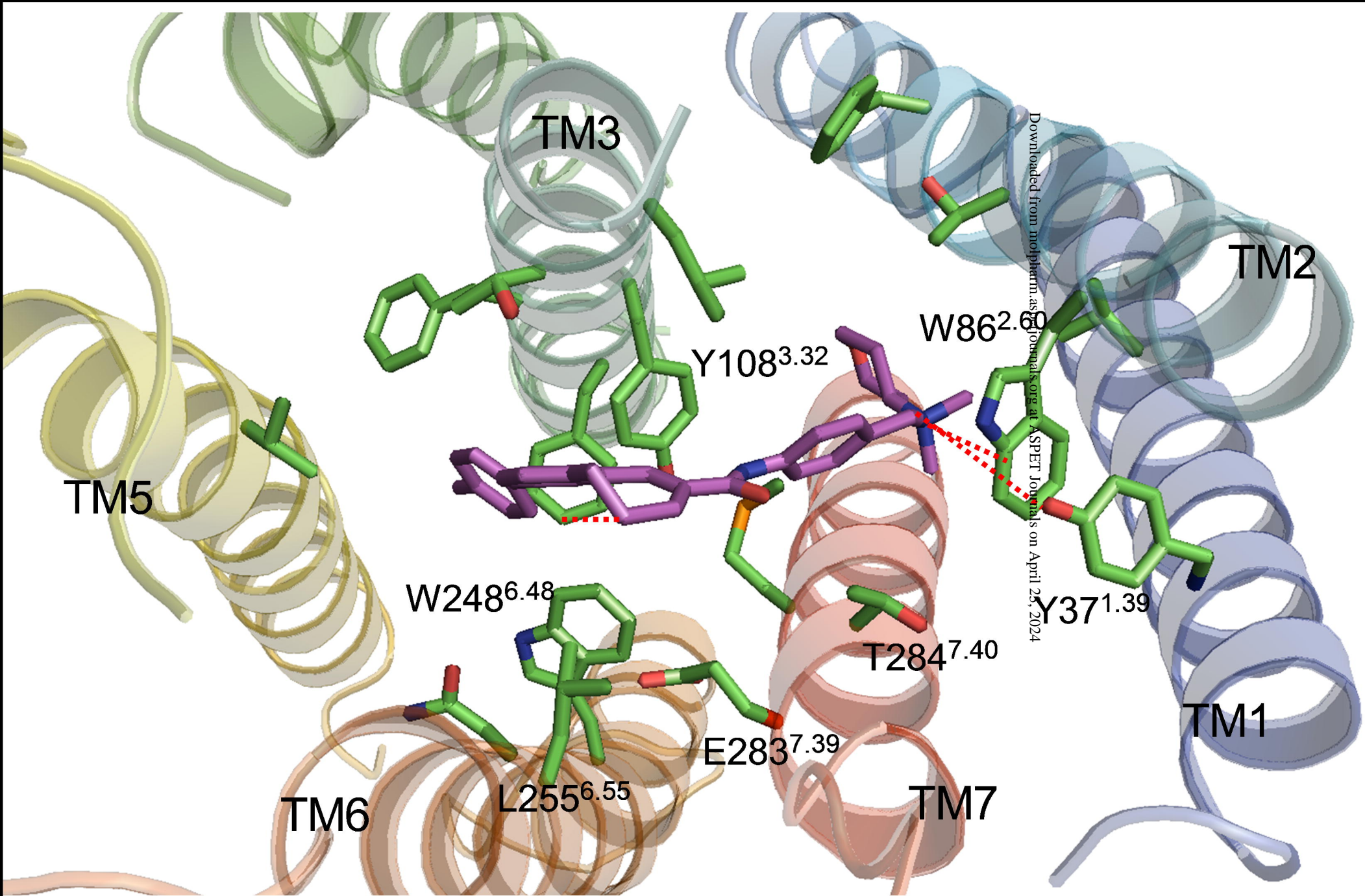


Figure 5C

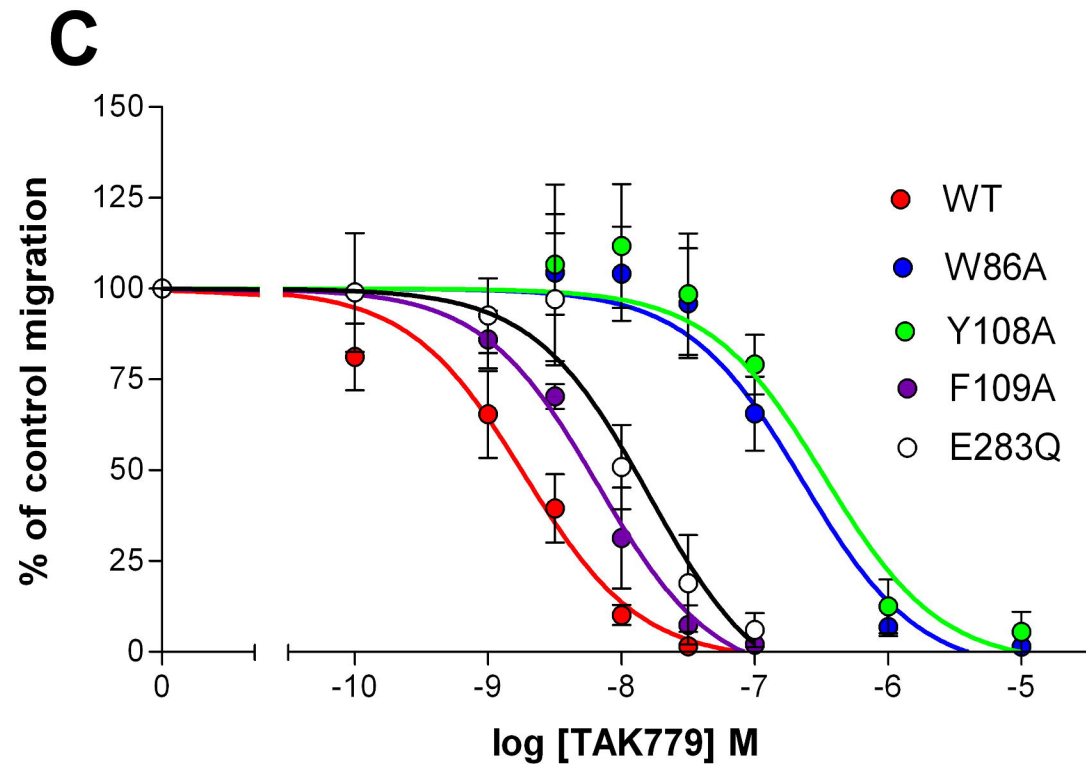
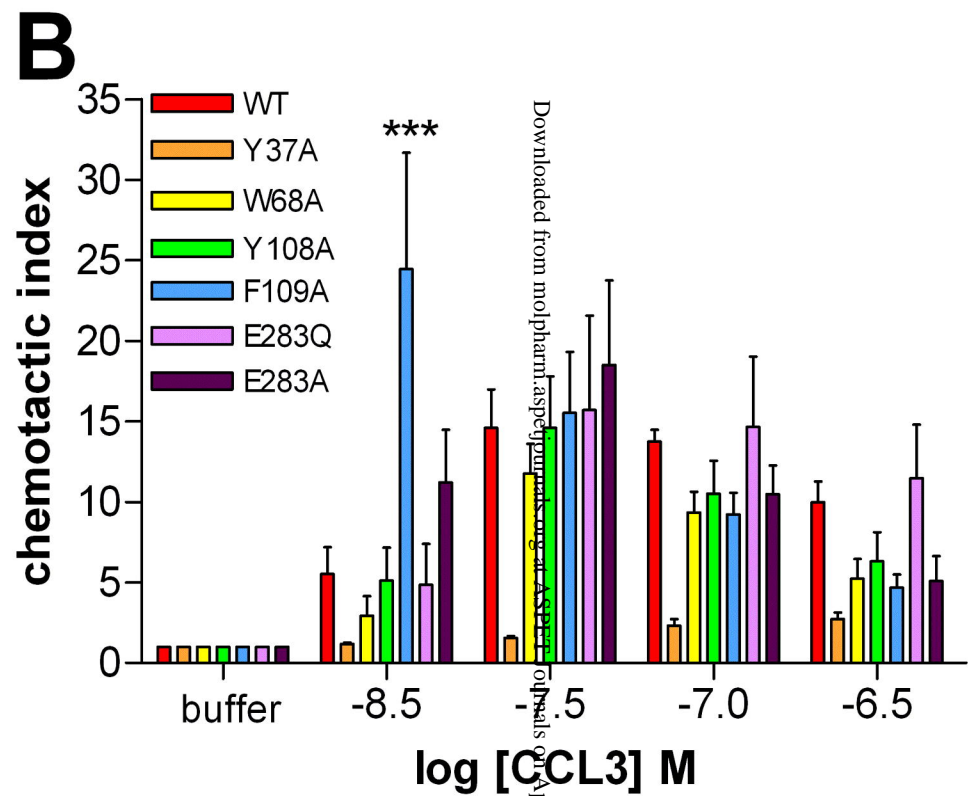
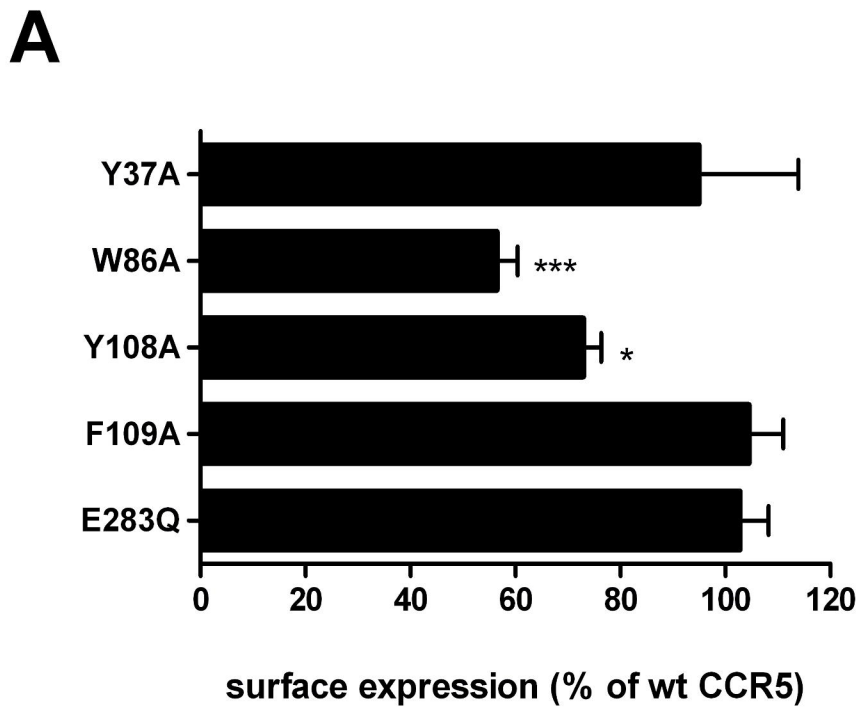


Figure 6